

DOT/FAA/AR-03/48

Office of Aviation Research
Washington, D.C. 20591

Assessment of Effects of Mixed-Phase Icing Conditions on Thermal Ice Protection Systems

May 2003

Final Report

This document is available to the U.S. public through the National Technical Information Service (NTIS), Springfield, Virginia 22161



U.S. Department of Transportation
Federal Aviation Administration

NOTICE

This document is disseminated under the sponsorship of the U.S. Department of Transportation in the interest of information exchange. The United States Government assumes no liability for the contents or use thereof. The United States Government does not endorse products or manufacturers. Trade or manufacturer's names appear herein solely because they are considered essential to the objective of this report. This document does not constitute FAA certification policy. Consult your local FAA aircraft certification office as to its use.

This report is available at the Federal Aviation Administration William J. Hughes Technical Center's Full-Text Technical Reports page: actlibrary.tc.faa.gov in Adobe Acrobat portable document format (PDF).

1. Report No. DOT/FAA/AR-03/48	2. Government Accession No.	3. Recipient's Catalog No.	
4. Title and Subtitle ASSESSMENT OF EFFECTS OF MIXED-PHASE ICING CONDITIONS ON THERMAL ICE PROTECTION SYSTEMS		5. Report Date May 2003	
		6. Performing Organization Code	
7. Author(s) Kamel Al-Khalil		8. Performing Organization Report No.	
9. Performing Organization Name and Address Cox & Company, Inc. 200 Varick Street New York, NY 10014		10. Work Unit No. (TRAIS)	
		11. Contract or Grant No.	
12. Sponsoring Agency Name and Address U.S. Department of Transportation Federal Aviation Administration Office of Aviation Research Washington, DC 20591		13. Type of Report and Period Covered Final Report	
		14. Sponsoring Agency Code AFS-220	
15. Supplementary Notes The Federal Aviation Administration Williams J. Hughes Technical Center COTR was Dr. James T. Riley.			
16. Abstract <p>The Federal Aviation Administration sponsored a preliminary experimental research program to study the effects of mixed-phase and fully glaciated icing conditions on the performance of thermal anti-icing ice protection systems (IPS). The experimental investigation was limited to a 36-inch chord NACA 0012 airfoil that was equipped with a leading-edge electrothermal ice protection system. The testing was accomplished at the Cox & Company, LeClerc Icing Research Laboratory tunnel, using the laboratory's newly developed capability to simulate mixed-phase icing conditions in their tunnel. Chordwise power required to operate the IPS in the evaporative mode (with an IPS surface temperature of 150°F) and in the running wet mode (with an IPS surface temperature of 50°F) was recorded with a model angle of attack of 0° and with supercooled liquid, mixed-phase, and glaciated conditions at temperatures of 0° and 12°F. Photographic records of the ice accretion and ice protection phenomena, using newly developed optical techniques, were obtained by the National Aeronautical and Space Administration Glenn Research Center Icing Branch. This report describes the test program and summarizes the associated results.</p>			
17. Key Words Snow, Artificial Snow, Anti-icing, Aircraft ice protection, Mixed-phase, Mixed-phase icing, Mixed-phase testing		18. Distribution Statement This document is available to the U.S. public through the National Technical Information Service (NTIS), Springfield, Virginia 22161	
19. Security Classif. (of this report) Unclassified	20. Security Classif. (of this page) Unclassified	21. No. of Pages 38	22. Price

ACKNOWLEDGMENTS

This program was sponsored by the Federal Aviation Administration (FAA) through a contract to Wichita State University (WSU), which in turn contracted to Cox & Company. Participation of the National Aeronautics and Space Administration (NASA) Glenn Research Center in this program, led by Mr. Dean Miller, provided valuable imaging techniques and recorded visualization, as well as droplet and particle identification, sizing, and equipment. Also, the model used for this investigation was fabricated and instrumented by Cox & Company for an earlier NASA Glenn Research Center-sponsored investigation. The current program would not have been accomplished without the prior Small Business Innovation Research sponsorship received from NASA Glenn for the development of the mixed-phase simulation capability at Cox. Recognizing the available resources, the current program was made possible by a recommendation from Mr. Eugene Hill, FAA National Resource for Aircraft Icing, and the technical leadership of Dr. James Riley, FAA William J. Hughes Technical Center. The support of WSU and the federal organizations that contributed to the successful completion of the investigation is well appreciated.

TABLE OF CONTENTS

	Page
EXECUTIVE SUMMARY	vii
1. INTRODUCTION	1
2. OBJECTIVES AND APPROACH	1
3. THE COX LIRL TUNNEL	3
4. ICING CLOUD SIMULATION	5
4.1 Snow Gun	5
4.2 Ice Shaver	5
4.3 Particle Size Characterization	6
4.4 Water Content Calibration	7
4.5 Cloud Generation	7
5. TUNNEL TEST SETUP	8
6. DATA ACQUISITION, CONTROL, AND MEASUREMENT UNCERTAINTY	10
7. ICING TUNNEL TESTS	10
7.1 Imaging and Visualization	12
7.1.1 Imaging Tools	12
7.1.2 Visual Results and Ice Traces	12
7.2 Thermal Tests	15
7.2.1 Repeatability	15
7.2.2 Evaporative Anti-Icing	20
7.2.3 Running-Wet Anti-Icing	25
8. CONCLUSIONS	28
9. REFERENCES	30

LIST OF FIGURES

Figure		Page
1	Layout of the Cox LeClerc Icing Research Laboratory Tunnel	3
2	Snow Gun in the Cox LIRL Tunnel	5
3	Ice Particle Imaging Using the OAP	6
4	Sample Snow Gun Particle Distribution	6
5	Sample Ice Shaver Particle Distribution	7
6	NACA 0012 Model (36" Chord) Installed in Test Station-2	9
7	Video Imaging Setup	9
8	Ice Particle Impact/Bounce Captured During Run 37	13
9	Erosion Effects on Ice Accretions in Rime Conditions	14
10	Erosion Effects on Ice Accretions in Glaze Conditions	14
11	Tunnel Sample Dry Data at 12°F	16
12	Tunnel Sample Dry Data at 0°F	17
13	Test Repeatability (Running-Wet, Shaver, 12°F)	18
14	Test Repeatability (Running-Wet, Mix-Gun, 0°F)	18
15	Test Repeatability (Evaporative, Mix-Gun, 0°F)	19
16	Test Repeatability (Evaporative, Shaver, 0°F)	19
17	Test Repeatability (Running-Wet, Mix-Shaver, 0°F)	20
18	Summary of Normalized Evaporative Total Power at 0°F	21
19	Evaporative Power Distributions at 0°F	23
20	Summary of Normalized Evaporative Total Power at 12°F	24
21	Evaporative Power Distributions at 12°F	24
22	Summary of Normalized Running-Wet Total Power at 0°F	25
23	Running-Wet Power Distributions at 0°F	26
24	Summary of Normalized Running-Wet Total Power at 12°F	27
25	Running-Wet Power Distributions at 12°F	27
26	Ice Ridge Formation Downstream of Heated Zone for Running-Wet System	28

LIST OF TABLES

Table		Page
1	Icing Test Conditions	11
2	Matrix of Icing Test Runs	11

EXECUTIVE SUMMARY

The Federal Aviation Administration sponsored a preliminary experimental research program to study the effects of mixed-phase (consisting of both supercooled liquid water drops and ice particles) and glaciated (consisting of ice particles only) on the performance of thermal anti-icing ice protection systems. The investigation was limited to a 36-inch chord NACA 0012 airfoil (a lifting surface) equipped with a leading-edge electrothermal ice protection system, with a model angle of attack of 0° . The ice protection system was simply set to off to investigate effects on unprotected surfaces. When set to on, the ice protection system was operated in evaporative and in running-wet modes. The effects of liquid, mixed-phase, and glaciated icing conditions on the power requirements of the ice protection system were measured. In addition, the National Aeronautics and Space Administration Glenn Research Center Icing Branch used newly developed optical techniques to record images of the icing and ice protection phenomena associated with the three classes of icing conditions for both unprotected and protected surfaces. No attempt was made to investigate the effects of mixed-phase or glaciated icing conditions on the performance of engines or air data system probes.

The testing included observation of ice accretion on unprotected (i.e., unheated) surfaces in glaciated clouds, mixed-phase clouds, and purely liquid clouds.

In glaciated conditions, ice accretion consisted only of a thin layer of frost visible on the surface with no further accumulation as time progressed. The layer was observed whether the ice particles were generated by the ice shaver or snow gun and is thought to be the residual of ice particles impacting the surface.

In mixed-phase icing conditions, the ice accretion resulted mainly from the supercooled water droplets present in the mixed-phase cloud. The effect of the ice particles depended on whether or not the icing conditions were rime conditions or glaze conditions.

In rime icing conditions, the ice particles in the mixed-phase clouds are not believed to have either augmented or significantly diminished the main ice accretion. The primary effect observed on the quantity of ice accreted was the erosion of feather-like ice growths aft of the main ice accretion. Also, the rime accretions in mixed-phase conditions tended to have an overall smoother appearance than rime accretions in purely liquid water conditions, which could have been due to a kind of sand-blasting effect by the ice particles.

In glaze icing conditions, the ice particles in the mixed-phase clouds are believed to have diminished the overall size of the ice accretion. This may have been due mainly to shedding or splashing of water from the surface water film due to ice particles bouncing in the film, and to a lesser extent, due to erosion of accreted ice by the incoming particles. Also, the accreted ice had an opaque white appearance with a slightly bumpy texture rather than the clear appearance characteristic of glaze accretions in a purely liquid water cloud. It is conjectured that this could have been due to impacting ice particles, leaving a residual that is trapped in the liquid layer or due to the smaller impacting particles sticking in the surface liquid film.

None of the test results suggested that ice accretions on unprotected surfaces in mixed-phase clouds would be more hazardous than those occurring in purely supercooled liquid water clouds. The accretions in mixed-phase clouds were, in general, found to be no larger, and sometimes smaller, than those in purely supercooled liquid water clouds with comparable liquid water content. They also tended to be smoother and with feathers and other protuberances absent or diminished in size.

Generally speaking, the performance of the evaporative thermal system on the model did not seem to be adversely affected by the presence of ice particles in the cloud. In fact, purely liquid clouds required more heat than mixed-phase or glaciated conditions with the same total water content. The lower power density requirements for the mixed-phase and glaciated conditions may have resulted from some of the ice particles bouncing from the surface without melting and from loss of water from the heater surface water film due to splashing caused by the impacting ice particles.

Ice protection systems operating at temperatures slightly higher than the freezing point of water, typical of running-wet systems, require less power than evaporative systems. This is because the aim is to prevent ice forming on the surface but not fully evaporating it. Running-wet power requirements increase as the ambient air temperature decreases. In mixed-phase icing conditions, additional power is required to offset the heat of fusion for melting the impinging ice particles. However, in this test, the large, relatively heavy, ice particles apparently cause shedding of the water film on the ice protection system surface through the dynamics of splashing as the ice particles strike and bounce from the airfoil's surface. The reduced water film thickness aft of the airfoil's stagnation point tended to offset the effects of the ice particles that impinge and adhere at the leading edge of the model. Consequently, the overall power required by the running-wet ice protection system was practically unchanged between all-liquid and mixed-phase conditions. However, in the running-wet mode of operation, the local power density was much higher around the stagnation area in the mixed-phase conditions compared to the purely liquid conditions. This is a result of the power required to offset the heat of fusion necessary to melt the impacting ice particles that either fully or partially stick to the surface. In all running-wet modes, runback ice was observed to freeze near the trailing edge of the protected surfaces, with the formation of an ice ridge resulting from the buildup of ice from subsequent runback water on initial runback ice formation.

Fully glaciated icing conditions did not adversely affect the overall power required by the ice protection system in either mode of operation (evaporative or running wet).

Results of this investigation do not resolve all questions concerning whether or not mixed-phase icing conditions are sometimes more hazardous to flight than purely liquid water conditions with the same liquid water content. Results of the current testing can be used by manufacturers to investigate the mixed-phase icing hazards associated with specific airplane components and designs. It would be valuable if this investigation were augmented to include additional testing parameters such as operational angle of attack, higher airspeed, and other total water content and liquid water droplet size. It is important to note that the effects on the operation of turbine engines and air data system probes remain to be investigated.

1. INTRODUCTION.

The safety of flight into mixed-phase (consisting of both supercooled liquid water drops and ice particles) and glaciated (consisting of ice particles only) atmospheric conditions has been a long-standing question, with limited scientific information available on which to base sound engineering decisions. Most information on in-flight icing is for purely supercooled liquid water clouds conditions, and certification requirements are written for those conditions. Experience has shown that glaciated and mixed-phase icing conditions can have deleterious effects on the operation of some turbine engines equipped with circuitous air induction systems, but little evidence exists that mixed-phase and glaciated icing conditions adversely affect the performance of airplane flying qualities or airframe ice protection systems. The National Transportation Safety Board has recommended to the Federal Aviation Administration (FAA) that Appendix C of Title 14 Code of Federal Regulations Part 25 be expanded to include mixed-phase icing conditions as necessary. Task 13C of the FAA Aircraft Inflight Icing Plan (April 1997) [1] stated that the FAA would conduct a study to determine the magnitude of the safety threat that is posed by mixed-phase conditions [2]. The FAA also tasked the Aviation Rulemaking Advisory Committee to define an icing environment and devise requirements to assess the ability of aircraft to safely operate without restriction in, or to safely exit from, mixed-phase icing conditions, if found to be more hazardous than the supercooled liquid droplet conditions with the same liquid water content.

The December 2-3, 1998, FAA Specialists' Workshop on Mixed-Phase and Glaciated Icing Conditions [3] addressed the climatology, measurement, characterization, and simulation aspects of mixed-phase and glaciated icing conditions. The issue of whether thermal ice protection systems should be designed for the total water content or only for the liquid water content of mixed-phase icing conditions was identified during the workshop. Icing cloud characterization research performed by various organizations indicates that mixed-phase conditions are relatively common in the atmosphere; results from the Meteorological Service of Canada indicated that approximately 40 percent of the icing encountered containing supercooled liquid drops also contained ice particles. The workshop also identified the potential hazards of ingestion of air from mixed-phase icing conditions by turbine engines and possible adverse effects of mixed-phase icing conditions on air data probes, such as total temperature and pitot probes.

The effect of these conditions on heated or unheated lifting surfaces has not been systematically evaluated and documented. To address this issue, the FAA sponsored a program to investigate the impact of mixed-phase and snow conditions on thermal ice protection systems (IPS). An exploratory test was conducted in the Cox & Company LeClerc Icing Research Laboratory (LIRL) tunnel in July 2002. This was a collaborative effort between the FAA, Wichita State University, Cox & Company, and NASA Glenn Research Center.

2. OBJECTIVES AND APPROACH.

The primary objective of this experimental program was to study the effects of mixed-phase and glaciated icing conditions on the performance of thermal IPSs on lifting surfaces. The secondary objective was to study the physics of ice particle behavior on protected (i.e., heated) and unprotected airfoil leading-edge surfaces (impact, bouncing, sticking, melting, etc.). A team of

engineers from the NASA Glenn Research Center carried out the visualization effort using state-of-the-art imaging tools and techniques.

The newly developed, unique capability to simulate mixed-phase and glaciated conditions in the Cox LIRL tunnel provided a means to accomplish the test objectives. The development of this testing capability by Cox & Company was accomplished through NASA Glenn Research Center, Small Business Innovative Research Phase I and Phase II awards.

A heated and instrumented airfoil model was used in these studies. The heated section consisted of multiple adjacent zones that were individually controlled, as described later. The model was previously developed for the NASA Code Validation Test Program that was conducted in the NASA IRT, as described in references 4, 5, and 6. The original airfoil model was trimmed from its original 6-ft span to 4-ft span to fit in Test Section-2 of the Cox LIRL tunnel. This test section was chosen to allow atomized water particles from the snow gun, described later, to be nearly fully frozen prior to impacting on the model's leading edge.

Testing was conducted with the heaters powered ON and OFF. The objective of keeping the heaters unpowered in some cases was to explore and document the icing physics on the surface, including ice particles impacting the surface, bouncing off, partially sticking, melting, etc. In the heaters ON cases, the objective was to document the changes in the surface icing physics and to determine the power required to maintain the surface at a certain preset temperature.

There are two anti-icing modes of operation for thermal IPS: evaporative and running wet. In the evaporative mode, the surface is heated to sufficiently elevated temperatures to evaporate the impinging ice/water particles and to prevent runback ice formation beyond the heated zone. This requires a surface temperature near or in excess of 120°F. In the running-wet mode, the surface is heated to prevent the impinging ice/water particles from freezing within the heated zone. This requires a surface temperature above 32°F. In practice, the temperature is held between 40° and 50°F. For electrothermal systems, this can be maintained with an appropriate controller. For hot/bleed air systems, it is more difficult to control, and the design is generally based on keeping the surface just above freezing at the coldest operating ambient temperature during icing conditions. This is typically at -22°F ambient air, per Appendix C of CFR Part 25.

To quantify the effects of ice/water content in the cloud on thermal IPS power requirements, many of the tests were conducted at the same total water content (TWC). The TWC is the sum of the supercooled liquid water content (LWC) and the frozen particles ice water content (IWC) in the cloud. The ratio of IWC to the TWC was varied between the different test conditions and included mainly 0%, 50%, and 100%. A few other cases of different ratios were also investigated. The IPS operation in the two different modes was conducted at the following temperatures:

- Evaporative anti-icing: surface near 150°F
- Running-wet power: surface near 50°F

The surface temperature in the evaporative mode was higher than normally used, 120°F. This was required as a result of the low air speed, which results in a low evaporation rate. Also, the

water film in the stagnation region has a greater tendency to bead up at low speeds and then runback, possibly to produce a frozen ridge beyond the heated zone.

In both heating modes, the power distribution and the total power were determined through a closed-loop control system. In the unheated cases, the surface physics and erosion effects of the incoming particles on the ice structure were studied and documented.

3. THE COX LIRL TUNNEL.

The Cox LIRL tunnel is a closed-loop icing wind tunnel, as shown in figure 1. There are two test sections: Test Section-1 is the smaller high-speed section just downstream of the contraction, and Test Section-2 is the larger low-speed section downstream of the first diffuser. Both sections are equipped with an air scavenge system for simulating engine inlets. The test sections have three heated windows for direct viewing and video or photographic recording of the test. The tunnel is constructed of steel and all major systems are acoustically treated and thermally insulated. The whole tunnel is isolated from the building using spring isolators and vibration-dampening pads.

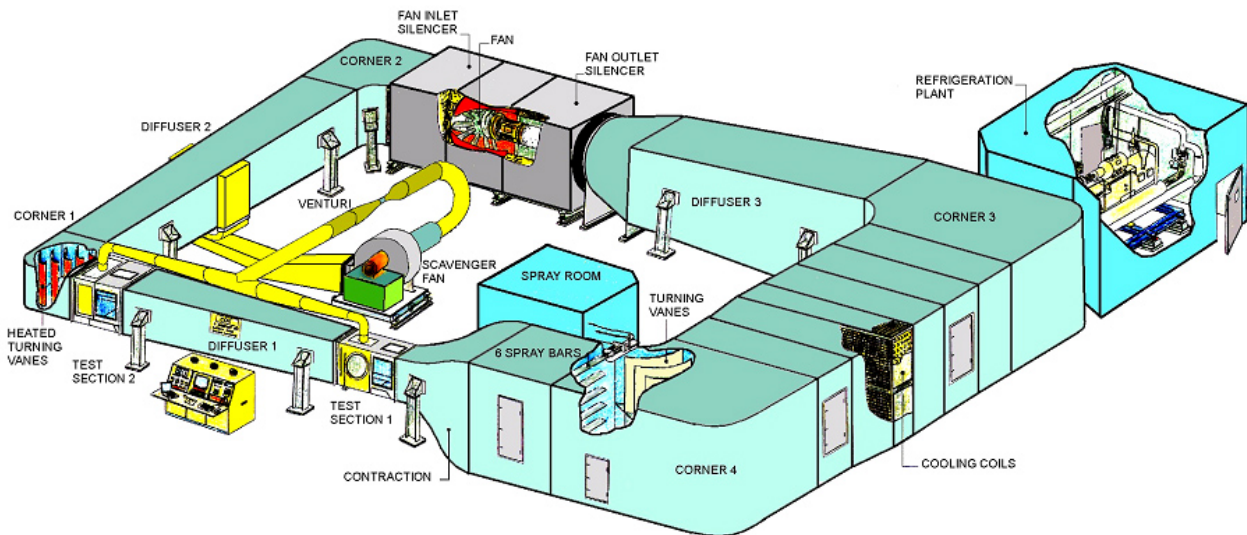


FIGURE 1. LAYOUT OF THE COX LeCLERC ICING RESEARCH LABORATORY TUNNEL

The supercooled water spray cloud is generated using spray bars obtained from NASA Glenn Research Center's Icing Research Tunnel. The spray drop size distribution and liquid water content is controlled by varying air and water pressures in the spray bars. The cloud was calibrated consistently in 1998 by NASA and in 2000 by Cox. Some general information about the Cox LIRL tunnel follows:

- Temperature envelope:
 - Minimum continuous cold at -22°F , at maximum air speed

- Test Section-1:
 - Dimensions: 28" wide, 46" high, 78" long
 - Typical maximum speed: 200 mph
 - Turntable for dynamic angle of attack variations
 - 3 heated viewing windows
- Test Section-2:
 - Dimensions: 48" wide, 48" high, 60" long
 - Maximum speed: 120 mph
 - 3 heated viewing windows
- Main drive system:
 - Drive motor: constant rpm, 200-hp A/C motor
 - Drive fan: 16-bladed axial fan, 72" diameter with pneumatically adjustable pitch for airspeed control
- Scavenge system for engine inlet flow:
 - Motor: 70-hp AC centrifugal fan motor
 - Control: variable frequency drive controller
 - Simulates engine inlet air flow of up to 13 lb/sec from either test section
- Refrigeration system:
 - Main compressor:
 - 80 tons of cooling capacity at -22°F, tunnel total temperature
 - 250-hp compressor motor
 - Secondary compressor with 100-hp motor can run independently for warm conditions or in parallel with the main compressor for high heat loads at the cold conditions
 - Condenser heat exchanger with water cooling tower
 - Evaporator heat exchanger face area: 10 x 15 ft
- Spraying system:
 - 6 horizontal spray bars
 - Up to 17 nozzle locations per bar (NASA type atomizing nozzles)
 - 360-psi water pump (water system filtration and deionizing)
 - 100-psi compressed air with 30 kW heater

4. ICING CLOUD SIMULATION.

The simulation of the different icing clouds was made possible by using a combination of ice or supercooled water. The latter was produced using the common spray bar method where filtered and de-ionized water was atomized using compressed heated air. The ice particles were produced using two different methods.

4.1 SNOW GUN.

Water was atomized through a nozzle using cold compressed air, as shown in figure 2. Due to the physical atomization process, water particles of close to spherical shapes are produced. The water particles are cooled during the expansion process of the nozzle-atomizing air. Most of the smaller particles freeze within a short distance from the nozzle exit. However, the larger particles require a longer time to release the energy associated with the latent heat of fusion in order to freeze. As a result, Test Section-2, being the farther from the snow gun, was chosen to allow a longer residence or hang time of the droplets before they strike the model.



FIGURE 2. SNOW GUN IN THE COX LIRL TUNNEL

4.2 ICE SHAVER.

Water was frozen in large ice blocks. Subsequently, these blocks were fed at a determined rate through a mechanical shaver that consisted of multiple rotating blades driven by a constant-speed motor. The shaved ice was then introduced into the freestream via a blower. The ice particles produced using this technique are usually irregular in shape and larger than those produced using the snow gun. Also, the particles are fully frozen as they are produced. Those generated using the snow gun required some residency time in the freestream to freeze prior to impacting the test model as discussed above.

4.3 PARTICLE SIZE CHARACTERIZATION.

Since differences in particle size and shape can affect trajectory and impact characteristics, it was desired to document particle features. A Particle Measuring Systems 2D-Grey optical array probe (OAP) was used to characterize details of ice particles from the snow gun and the ice shaver. The instrument was installed such that the measuring location coincided roughly to the mid-span of the heated test model. Calibration tests were conducted prior to airfoil model installation and testing. Sample ice particle images from the snow gun and the ice shaver, as captured by the OAP, are shown in figure 3. Example results of particle size distribution are shown in figures 4 and 5 for the snow gun and ice shaver, respectively. Corresponding median volume diameters (MVDs) in these figures were approximately 150 and 185 microns, respectively. In general, the ice shaver produced larger particles with an MVD near 200 microns.

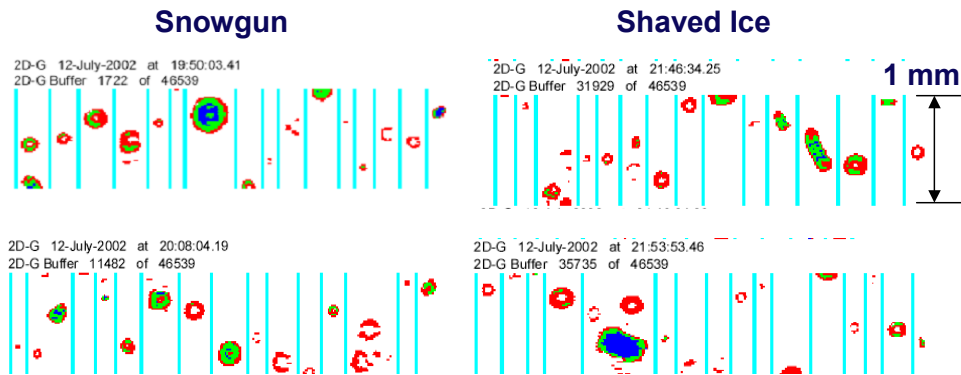


FIGURE 3. ICE PARTICLE IMAGING USING THE OAP

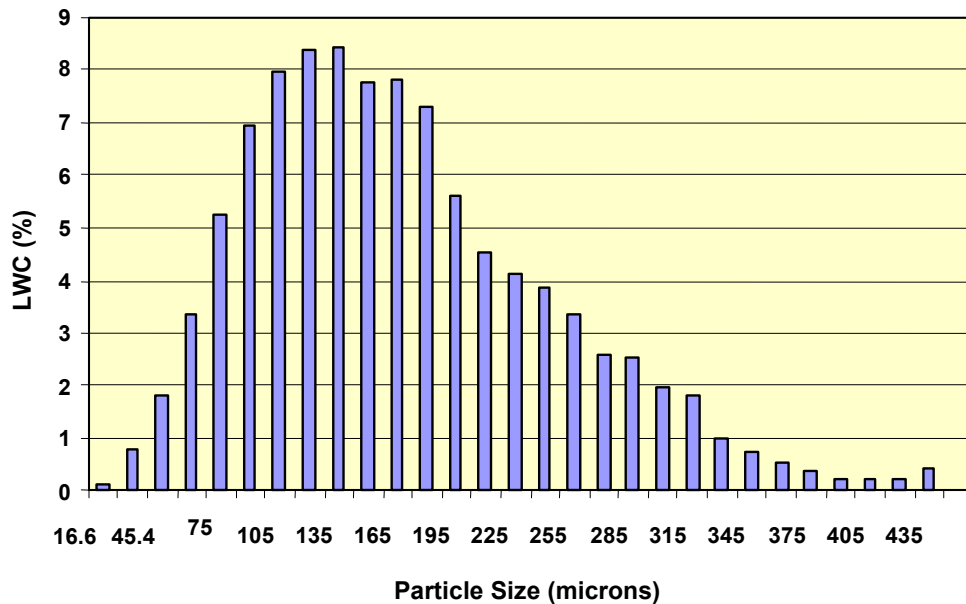


FIGURE 4. SAMPLE SNOW GUN PARTICLE DISTRIBUTION

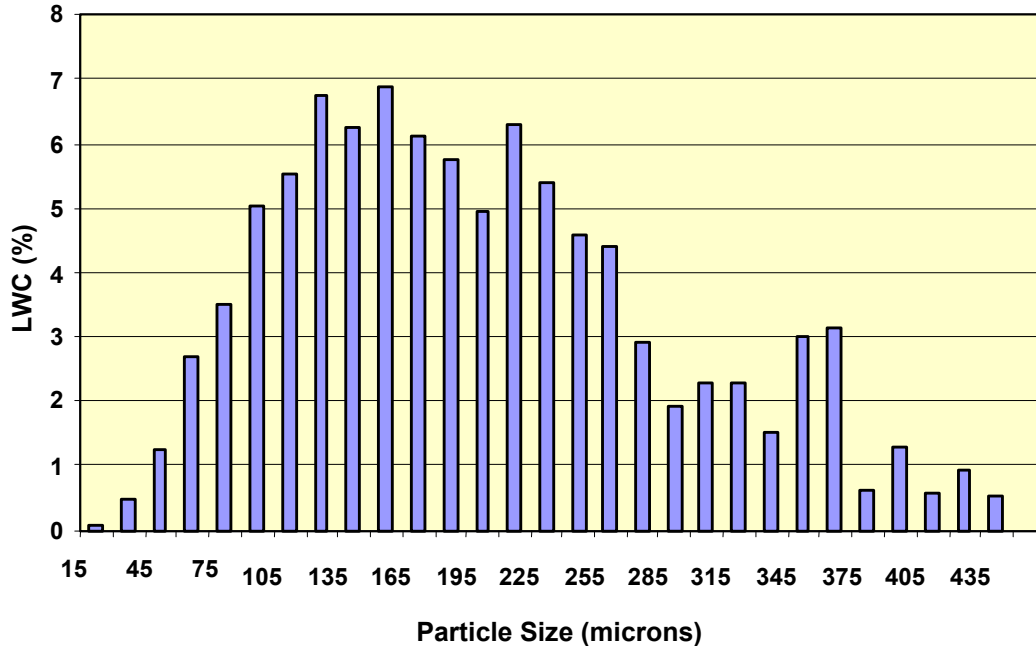


FIGURE 5. SAMPLE ICE SHAVER PARTICLE DISTRIBUTION

4.4 WATER CONTENT CALIBRATION.

The IWC using the snow gun or the ice shaver was calibrated prior to installation of the test model. This was accomplished using the Nevzorov TWC instrument, which consists of two sensors: (1) a LWC sensor and (2) a TWC sensor. The IWC is computed from the difference between the TWC and the LWC. Generally, the IWC is slightly underestimated since the LWC sensor has some thermal response from ice particles. Theoretically, these ice particles are assumed to bounce off that sensor, regardless of the size. Ice particles are assumed to be collected, along with water particles, on the TWC sensor. This does not account for some ice particles bouncing off the TWC sensor, especially in the fully glaciated conditions. Correspondingly, the IWC might be slightly underestimated. The overall accuracy of the Nevzorov probe has been accepted within the community of icing and cloud characterization researchers. It certainly meets the purpose of this test program.

4.5 CLOUD GENERATION.

The icing cloud generated in the tunnel is artificially simulated using different techniques for the different types of icing conditions. These are summarized as follows.

- Supercooled: The normal tunnel spray bars are used for this purpose where compressed air is used to atomize pressurized water using NASA type nozzles (MOD-1).
- Glaciated: Two different methods are used to produce glaciated icing conditions as explained earlier:

- Snow Gun: Air-assisted atomization and freeze-out of water particles.
- Ice Shaver: Mechanically shaving frozen ice blocks and dispersing the ice particles in the freestream using a blower.
- Mixed: Mixed conditions are defined as icing clouds where supercooled liquid water droplets co-exist with frozen ice particles. Consequently, the corresponding amount of LWC and IWC is produced using the appropriate methods described in the previous paragraphs. Thus, a mixed-phase condition can be produced using one of the following two combinations:
 - Supercooled (spray bars) + ice particles using the ice shaver
 - Supercooled (spray bars) + ice particles using the snow gun

5. TUNNEL TEST SETUP.

All tests in this program were conducted in Test Section-2 where the speed is limited to 120 mph. This section was chosen to insure that the great majority of ice particles produced using the snow gun were fully frozen. Only the largest particles, those at the upper end of the size distribution of atomized particles in the tunnel cloud, would be partly liquid, and even they would be nearly fully frozen. The goal was to obtain additional information from effects of ice particle size and shape using the two different simulation methods (snow gun and ice shaver).

The airfoil was mounted horizontally in Test Section-2, as shown in figure 6. All tests were conducted at a single angle of attack (zero degree) due to the extent of the tasks to be accomplished within the limited time period. A detailed description of the 3-ft chord by 4-ft span NACA 0012 heated airfoil model is provided in reference 4. It consisted of 14 individually powered and controlled heater zones. The layout and numbering of the heaters is shown in figure 6. Seven heaters were duplicated spanwise for redundancy. Additionally, due to the airfoil symmetry and zero degree flow angle of attack, top and bottom redundancy resulted.

The model was fitted with several sensors. Only those that measured the surface temperature near the mid-span were used to acquire data and control the heater power. These were located at ± 4.5 inches on either side of the mid-span, centered within each heater streamwise extent.

The video imaging setup is shown in figure 7. Three cameras were used to image the leading edge of the test article.

- A high-definition (HD) video camera and recorder were used to capture close-up details of ice particle impact in high resolution.
- A high-speed close-up camera to allow slow motion analysis of impact (Phantom V High-frame rate).
- A mini-digital video camera with a wide field of view to provide context for the other two cameras.

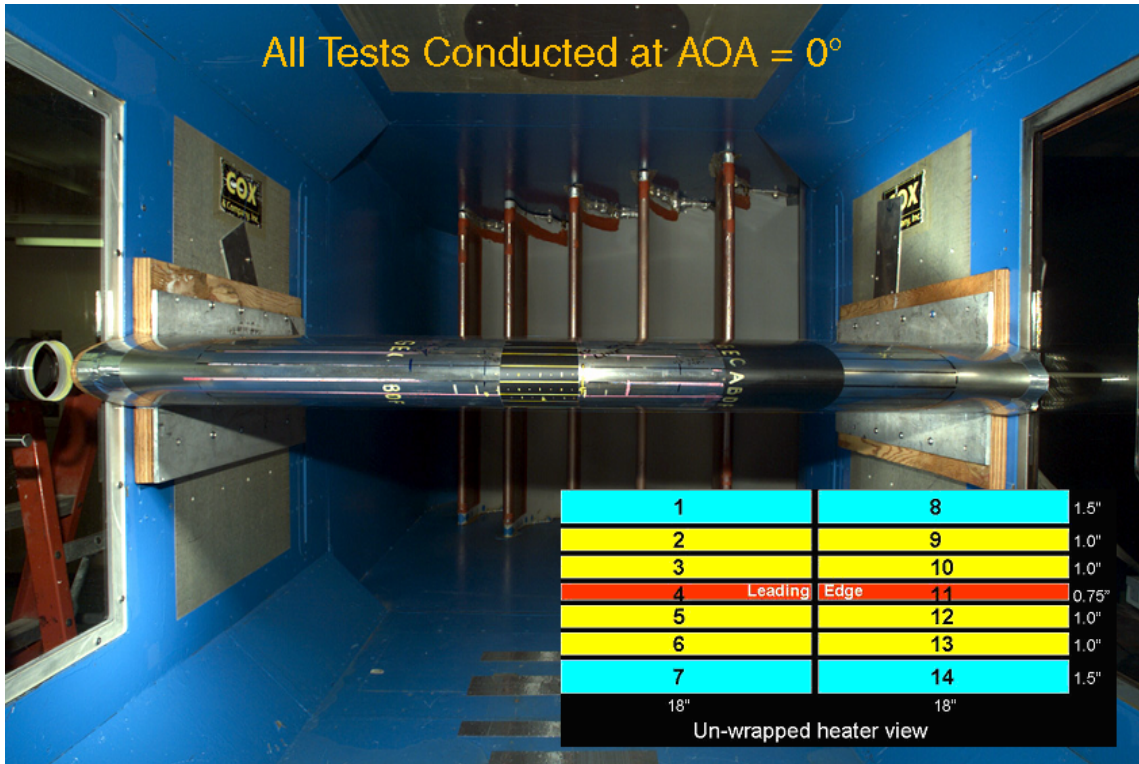


FIGURE 6. NACA 0012 MODEL (36" CHORD) INSTALLED IN TEST STATION-2

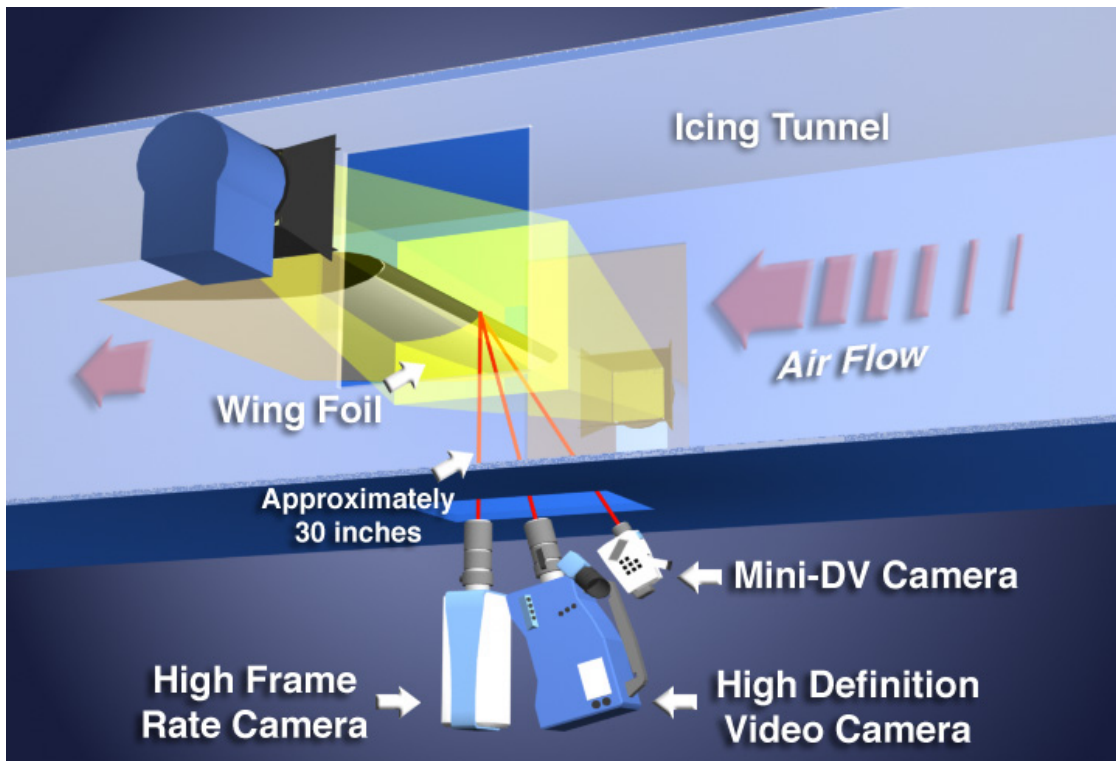


FIGURE 7. VIDEO IMAGING SETUP

6. DATA ACQUISITION, CONTROL, AND MEASUREMENT UNCERTAINTY.

The Cox Thermal Test Management System (TTMS) was used to power the 14 heated zones and record the data. The TTMS is a computer-based test management and data acquisition system. Power was regulated to each particular zone to maintain the specified constant surface temperature for each of the two anti-icing modes of operation (evaporative and running wet).

In most cases, the TTMS modulated the power below 100% duty cycle to maintain the surface at 50°F in the running-wet modes. However, the hilite heaters (nos. 4 and 11) were running at full power in evaporative cases as well as in several running-wet cases. The corresponding surface temperature was lower than the preset values, but higher than the freezing temperature. Specific details are discussed in section 7.

The test model was used during a previous test program (NASA Code Validation) as indicated in references 4 through 6. The instrumentation uncertainty for temperature measurements, using the thermocouples, were estimated by Miller, et al. [4]. In an attempt to estimate this uncertainty, three potential uncertainty factors were considered:

- Positional uncertainty
- Measurement uncertainty introduced by the data acquisition process
- Uncertainty due to the sensor's inherent accuracy

As a result of this uncertainty analysis, the surface temperature measurements were estimated to be $\pm 3^\circ\text{F}$ at a surface heat flux of 10 W/in^2 . This uncertainty can be as high as $\pm 8^\circ\text{F}$ at a surface heat flux of 30 W/in^2 . The latter high value of heat flux was typical of heaters at the stagnation region (heaters 4 and 11) in all evaporative cases as well as any mode (evaporative or running wet) when in mixed-phase icing conditions. This will be shown in section 7 where the results are discussed. Since the temperature is controlled in a closed loop, the uncertainty in the thermocouple produces an uncertainty in the heat flux obtained from the controller. The uncertainty in the measured heat flux is estimated to be less than 1 W/in^2 at 10 W/in^2 and less than 2.5 W/in^2 at 30 W/in^2 .

7. ICING TUNNEL TESTS.

Testing was conducted at various environmental conditions. Table 1 lists the icing test conditions explored. Generally, a mid-range ambient temperature (12°F , near glaze) and a cold ambient condition (0°F , rime) were considered. All tests were run at 120 mph and zero degree angle of attack. Generally, the TWC was near 0.7 g/m^3 . Other variations were also explored. The list of icing runs is shown in table 2 where the associated icing test condition in each run is referenced from table 1. Table 2 also indicates the IPS heater mode of operation in each run. The duration of the icing test in all the runs was near 10 minutes or until stable results were obtained.

TABLE 1. ICING TEST CONDITIONS

Icing Test Condition	True Air Speed (mph)	Total Temp. (°F)	Spraybar*	Snow Gun	Ice Shaver	TWC (g/m ³)
			LWC (g/m ³)	IWC (g/m ³)	IWC (g/m ³)	
Warm						
1	120	12	0.70			0.70
2	120	12	0.35	0.35		0.70
3	120	12	0.30	0.70		1.00
4	120	12	0.70	0.30		1.00
5	120	12	0.35		0.35	0.70
6	120	12			0.70	0.70
7	120	12		0.70		0.70
Cold						
8	120	0	0.70			0.70
9	120	0	0.35	0.35		0.70
10	120	0	0.35		0.35	0.70
11	120	0			0.70	0.70
12	120	0		0.70		0.70
13	120	0		0.30		0.30
Warmest (Tracings Only)						
14	120	22	0.70			0.70
15	120	22	0.70		0.70	1.40

*Supercooled water droplets, MVD = 20 microns

TABLE 2. MATRIX OF ICING TEST RUNS

Tunnel Run No.	Icing Test Condition	IPS Thermal Condition	Tunnel Run No.	Icing Test Condition	IPS Thermal Condition
7/16/2002			7/18/2002 (continued)		
1	6	Off	24	9	Off
2	6	Off	25	8	Evaporative
3	5	Off	26	8	Running-wet
4	5	Off	27	11	Evaporative
5	1	Off	28	11	Running-wet
6	11	Off	7/19/2002		
7	10	Off	29	2	Evaporative
8	8	Off	30	2	Running-wet
7/17/2002			31	7	Evaporative
9	14	Off	32	7	Running-wet
10	15	Off	33	9	Evaporative
11	1	Evaporative	34	9	Running-wet
12	1	Running-wet	35	12	Evaporative
13	5	Evaporative	36	12	Running-wet
14	5	Running-wet	37	10	Evaporative
15	6	Evaporative	38	10	Running-wet
16	6	Running-wet	39	10	Off
17	6	Running-wet	40	13	Evaporative
7/18/2002			7/23/2002		
18	2	Off	41	12	Evaporative
19	3	Off	42	12	Running-wet
20	4	Off	43	9	Off
21	7	Off	46	12	Evaporative
22	13	Off	44	11	Evaporative
23	12	Off	45	11	Running-wet

7.1 IMAGING AND VISUALIZATION.

A key component of this investigation was the close-up imaging of the ice particle impact. This work was performed by members of the Icing Branch and the Imaging Technology Center from NASA Glenn Research Center. The intent of the visualization effort was to provide close-up visual information about the ice particle impact, which could complement the thermal measurements. It was hoped that close-up imaging could provide qualitative insight into the physics of the impact process, and the degree to which ice particles stick or bounce for particular mixed-phase tunnel and test article surface conditions.

7.1.1 Imaging Tools.

An HD video camera was selected as the primary tool for close-up imaging of ice particle impact because of its extremely high-resolution capabilities. These qualities were identified during an earlier test entry in the Cox LIRL tunnel.

A Phantom V high-frame rate camera was used during a portion of the mixed-phase test to capture high-speed images of ice particle impact. Though this camera does have the capability to provide quantification of captured imagery, this type of analysis was not performed on the data acquired during the mixed-phase test. The captured imagery provides slowed down sequences, which facilitate qualitative analyses of the impact process.

A third camera, a mini-DV camera, was also used during the mixed-phase test to provide a wider field of view on the test article. Its wider field of view was needed to put the close-up imagery of the HD and Phantom cameras in proper context with respect to what was being observed elsewhere on the model.

A detailed analysis of the visualization data from the cameras was not performed when this report was generated. These data are archived at NASA for future analysis or test planning. However, general observations about the data are referred to in this document.

7.1.2 Visual Results and Ice Traces.

Bouncing ice particles were observed in all runs, with a heated or unheated surface, and with or without a supercooled liquid water spray. With the current visualization and imaging instruments, it is not yet possible to quantify the amount of particles that bounce off the surface. Figure 8, taken with the Phantom V high-frame rate camera, illustrates a snapshot of these effects as captured during run 37 (condition 10).

In the case of unheated tests in glaciated conditions, only a thin layer of frost was visible on the surface with no further accumulation as time progressed. This layer is thought to be the residual of ice particles impacting the surface. This observation was made regardless of whether the ice shaver or the snow gun was used. In mixed-phase unheated conditions, supercooled liquid and ice particles in the cloud, the phenomenon of erosion was observed on the accreted ice. These effects were temperature dependent. The following discussion illustrates this point.

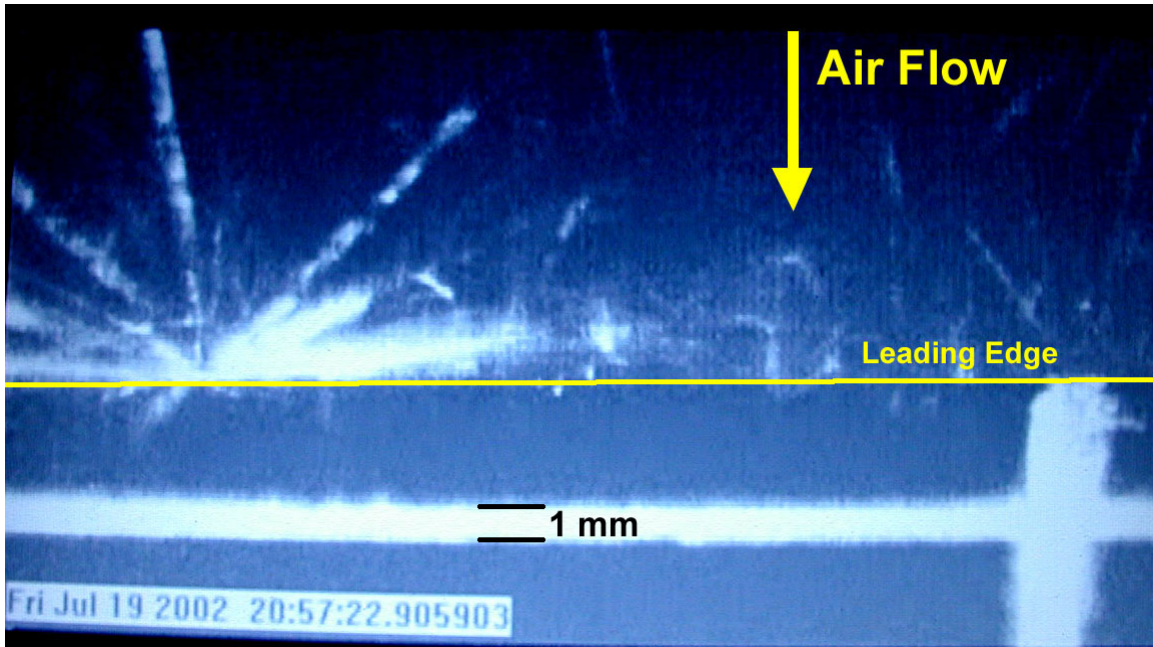


FIGURE 8. ICE PARTICLE IMPACT/BOUNCE CAPTURED DURING RUN 37

Figure 9 illustrates the effect of erosion on accreted ice in mixed rime icing conditions. These correspond to runs 19 and 20. Based on the known conditions and collection efficiency of the supercooled water droplets, it is apparent that the ice shapes were a result of the supercooled water droplets in the mixed cloud. The existence of the ice particles in the mix did not seem to significantly affect the amount of accreted ice for the given LWC. The only noticeable effect of the ice particles was the erosion of the feather-like ice growths close to the impingement limits. Compared to near the stagnation region, the collection efficiency is very low near the impingement limits, and the high local tangential speeds may cause increased erosion of the accretions. At this cold temperature, the impact of ice particles in the stagnation region does not significantly reduce the rime ice that accretes. However, further downstream, the bombardment by the solid and relatively heavy ice particles removes the ice feathers as a result of the scraping phenomenon associated with the high momentum (speed and size) and the grazing angle. The feathers are thin individual nodules that can be cracked off the surface much more easily and with less force than equivalent mass spread relatively smoothly over the surface, as is the case in the stagnation region. The rime accretions tended to have an overall smoother appearance in the mixed-phase rime conditions due to the sand-blasting effects of the ice particles.

In mixed-phase glaze icing conditions, erosion effects were clearly more significant. Two cases were conducted at 22°F, which illustrate these effects. Figure 10 illustrates ice tracings from runs 9 and 10. In run 9, only supercooled liquid water at 0.7 g/m^3 was used. The clear ice accumulation at the stagnation region and the beginning formation of horns away from the stagnation was an indication of glaze ice accretion where the freezing fraction was less than unity. In run 10, 0.7 g/m^3 of frozen ice particles were added to the cloud, producing a TWC of 1.4 g/m^3 . Surprisingly, the accreted ice was diminished instead of growing larger. The ice feathers and horns disappeared compared to the previous case. In addition, a slight reduction in accreted ice around the stagnation area is visible from the tracings. This could be caused by a

combination of erosion and splashing of the existing liquid layer in that area due to the low freezing fraction.

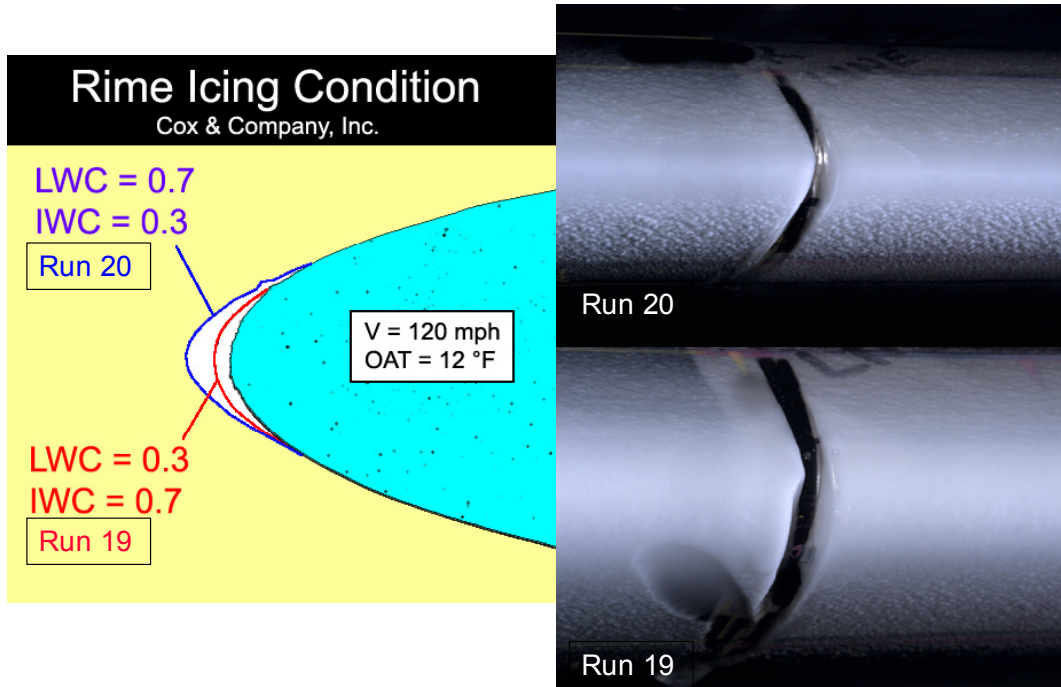


FIGURE 9. EROSION EFFECTS ON ICE ACCRETIONS IN RIME CONDITIONS

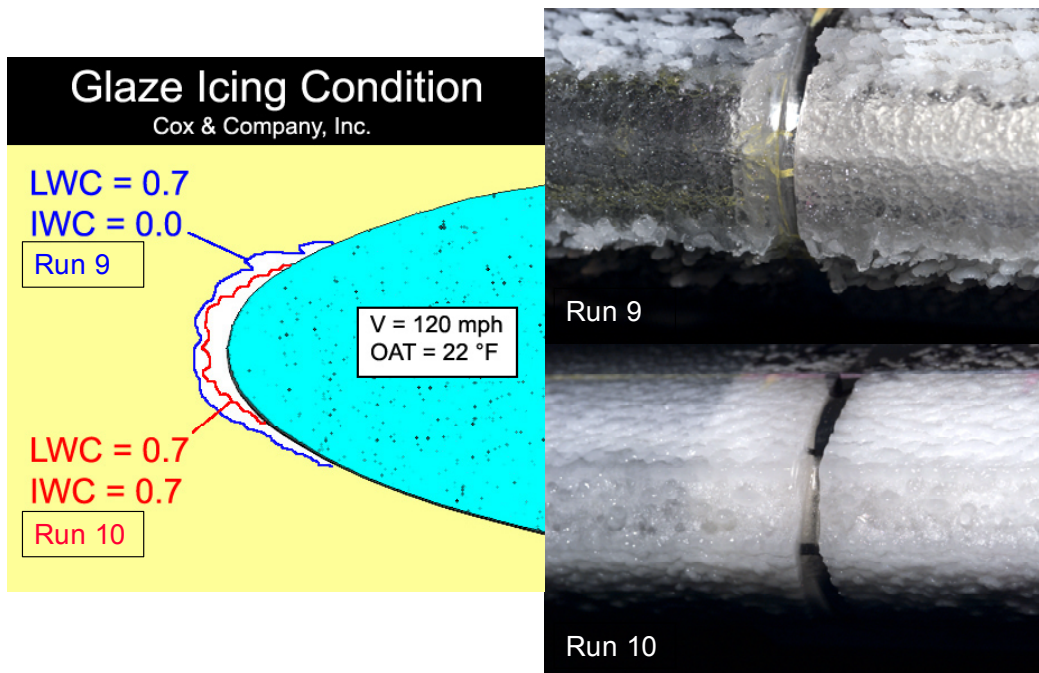


FIGURE 10. EROSION EFFECTS ON ICE ACCRETIONS IN GLAZE CONDITIONS

Interestingly, the accreted ice in these glaze conditions changed from clear to opaque white as in the rime cases with a slight bumpy texture. The explanation could be that impacting ice particles leave residuals that get trapped by the liquid layer. In addition, the smaller ice particles within the distribution may actually stick to the surface when a liquid layer exists. In rime cases, the supercooled water droplets freeze on impact, leaving a smooth hard surface for ice particles to strike and bounce off. The physics are similar to the fully glaciated icing conditions where ice particles bounce off the hard metal leading edge.

When the surface was heated, significant liquid water was observed on the surface around the stagnation region in evaporative cases and over the entire heated region and beyond in running-wet cases. This was observed whether the icing conditions were due to all-liquid supercooled water, mixed-phase, or fully glaciated conditions. The results for the fully glaciated conditions indicate that ice will stick, at least partially, to heated surfaces. The video images showed particles bouncing, but the amount could not be quantified with current imaging tools. The thermal data that follow will illustrate the increase in power requirements due to mixed or glaciated icing conditions near the stagnation area. Also, splashing is another phenomenon observed that could not be readily quantified.

7.2 THERMAL TESTS.

Due to the large volume of data to be presented, cases for the two different ambient temperatures will be discussed separately. However, It will be shown that the colder conditions were more severe, requiring more power, than the warmer conditions for the same cloud conditions.

The total power was computed for all heaters for the following conditions:

- Evaporative at 0°F ambient
- Evaporative at 12°F ambient
- Running-wet at 0°F ambient
- Running-wet at 12°F ambient

7.2.1 Repeatability.

The validity of the thermal data relies on the following:

- Accuracy of the tunnel simulation capability of the various conditions
- Model design and instrumentation
- TTMS data acquisition and control

The repeatability of the tunnel simulation capability in supercooled liquid water conditions has been established over the last several years. Considering that the mixed-phase simulation is a new addition to the tunnel simulation capabilities, its accuracy will have to be proven by repeated testing over the next few months or years. However, the following results indicate that the data is meaningful and predictable in relation to the corresponding conditions.

7.2.1.1 Dry Conditions.

A dry heated test is a very good measure of repeatability of certain tunnel conditions (airspeed and temperature), the model instrumentation, and the TTMS data acquisition and control system. In most runs, the power to the model was controlled and the surface temperature stabilized to evaporative conditions (150°F). The individual heater powers were measured by the TTMS. The resulting data was used to compute the external heat transfer coefficient for each heater. Results are shown in figures 11 and 12 corresponding to the 12°F and 0°F ambient temperatures, respectively. It is clear that the results are very consistent between all the different runs, with only slight variations at the aft-most heaters (nos. 1, 7, 8, and 14). Reference to figure 6 is advised for the heaters layout and nomenclature. The slight nonsymmetry in the results is associated with the hilite heaters (nos. 4 and 11) being offset chordwise by as much as 0.1 to 0.18 inch from the hilite. An increase in the heat transfer coefficient was noticed at the aft-most heater locations. The most probable cause for this behavior is transition of the flow from laminar to turbulent.

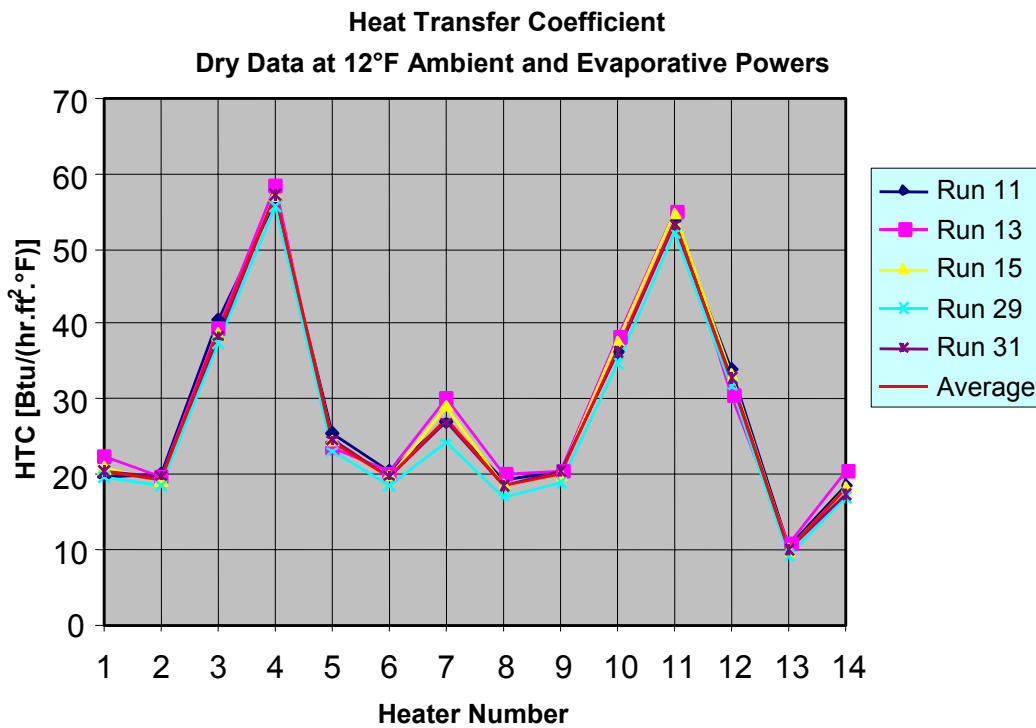


FIGURE 11. TUNNEL SAMPLE DRY DATA AT 12°F

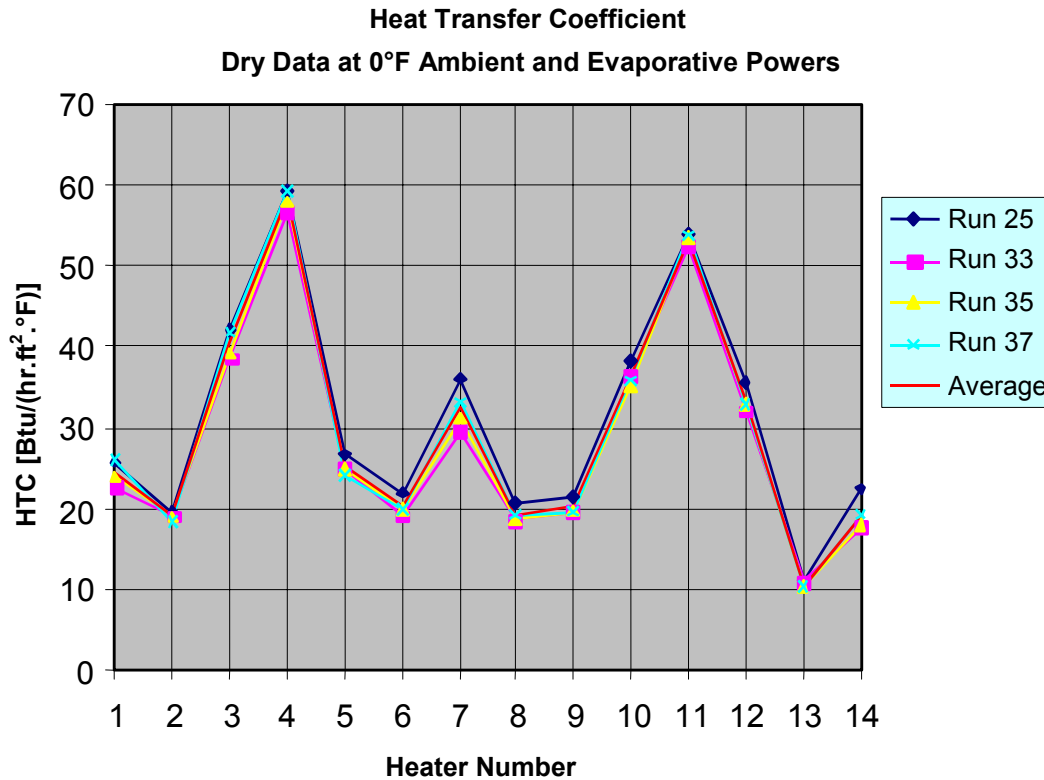


FIGURE 12. TUNNEL SAMPLE DRY DATA AT 0°F

7.2.1.2 Wet Conditions.

To establish the consistency of the tunnel test conditions as well as the thermal test setup and controls in the wet conditions, a few runs were repeated at the same conditions. Recall that heaters 8 through 14 are redundant to heaters 1 through 7 (figure 6). Also, because of the flow symmetry and zero degree angle of attack, results presented in the remainder of this document are averages of the corresponding redundant and symmetric heaters. In the following comparisons, the power density distribution (W/in^2) is plotted versus heater location.

The first repeat was run 17, which followed run 16. This is a running-wet anti-icing mode at an ambient temperature of 12°F in a fully glaciated icing condition using the ice shaver to produce the ice particles. Results shown in figure 13 are within the expected variance. All other repeats, runs 41 through 45 in table 2, were performed on the week following the end of the test program. Figure 14 illustrates the repeatability between runs 36 and 42. This is a running-wet anti-icing mode at an ambient temperature of 0°F in a mixed-phase icing condition, where the ice particles were generated using the snow gun. The equivalent test condition was repeated in an evaporative anti-icing mode. The corresponding results are shown in figure 15 for runs 35 and 41. Again, the repeatability looks very good.

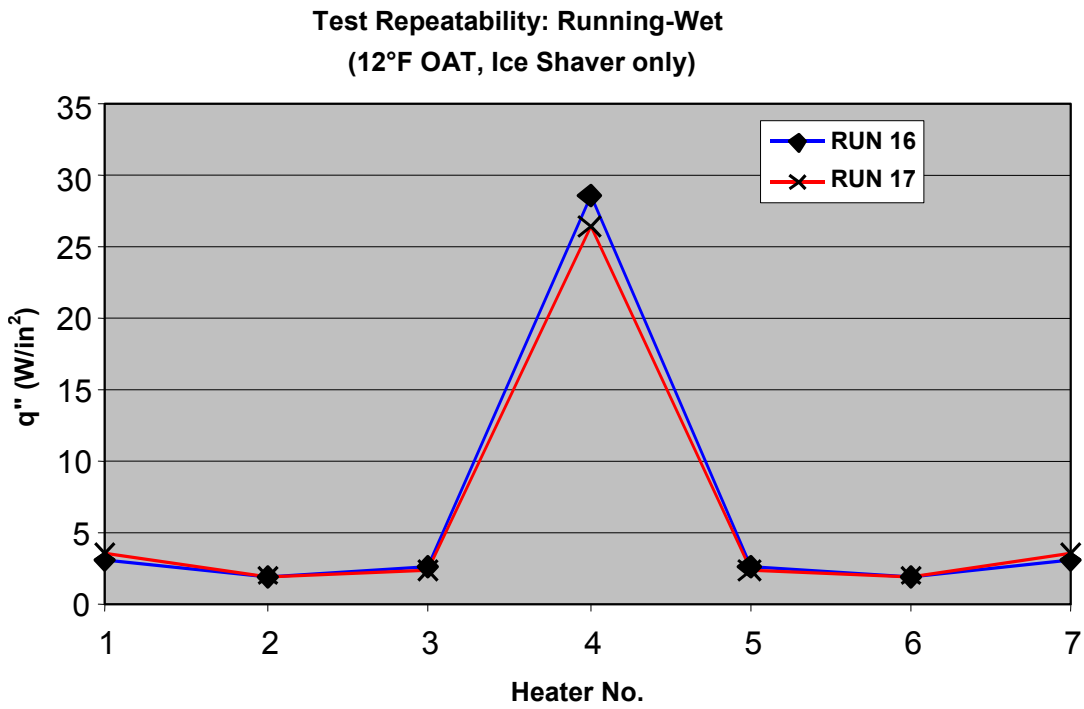


FIGURE 13. TEST REPEATABILITY (RUNNING-WET, SHAVER, 12°F)

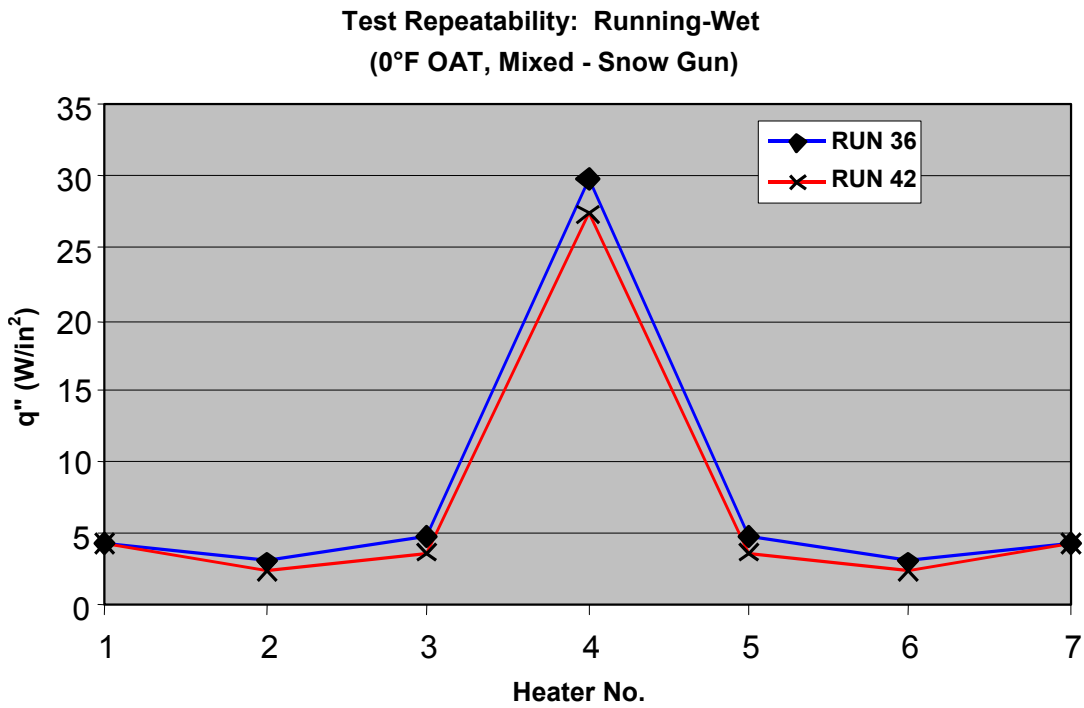


FIGURE 14. TEST REPEATABILITY (RUNNING-WET, MIX-GUN, 0°F)

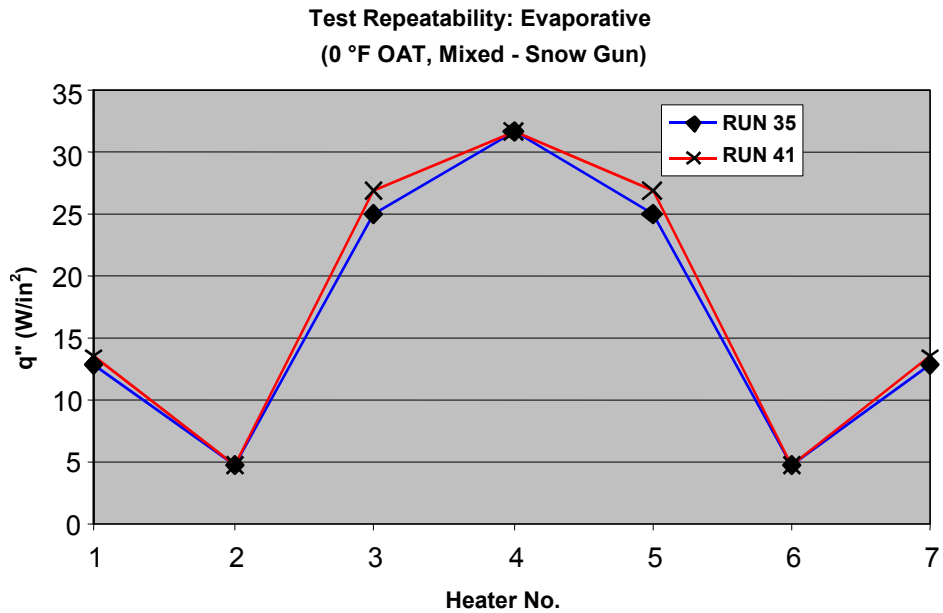


FIGURE 15. TEST REPEATABILITY (EVAPORATIVE, MIX-GUN, 0°F)

Another condition corresponding to an evaporative anti-icing mode at an ambient temperature of 0°F in a fully glaciated icing condition, using the ice shaver to produce the ice particles, was repeated. Results are shown in figure 16, corresponding to runs 27 and 44. The main difference in results between these two runs is at the heaters just downstream of the stagnation heater. The local difference might seem large. However, the difference between the total integrated heating powers for each of these two runs is less than 5%.

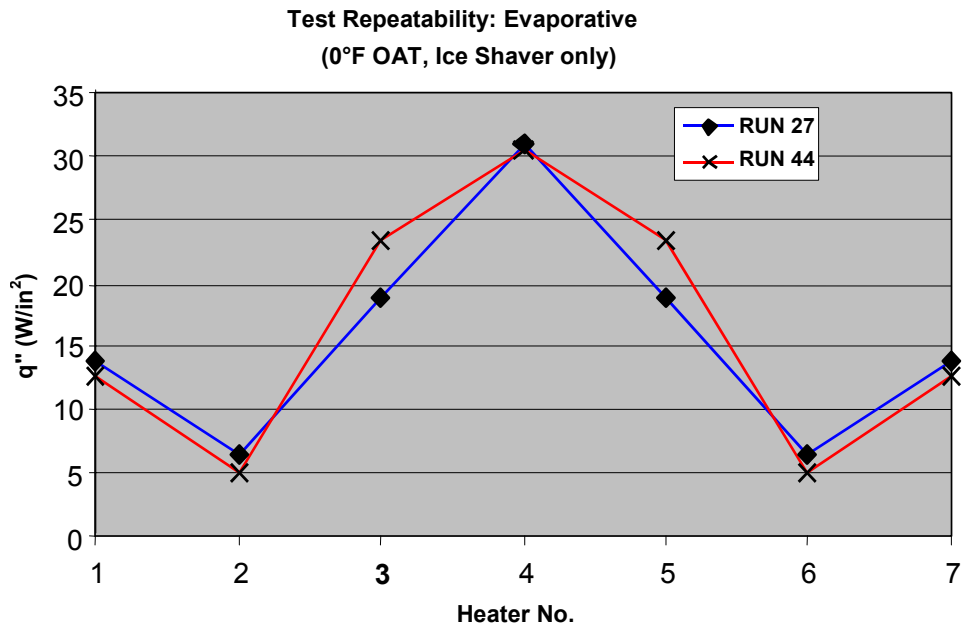


FIGURE 16. TEST REPEATABILITY (EVAPORATIVE, SHAVER, 0°F)

The last repeat run corresponds to a running-wet anti-icing mode at an ambient temperature of 0°F in a mixed-phase icing condition where the ice particles were generated using the ice shaver. Results are shown in figure 17 for runs 28 and 45. This is similar to the case shown in figure 14 where the snow gun was used instead. The repeatability of the results looks very good. A summary of the test results is shown in the following sections for evaporative and running-wet anti-icing modes.

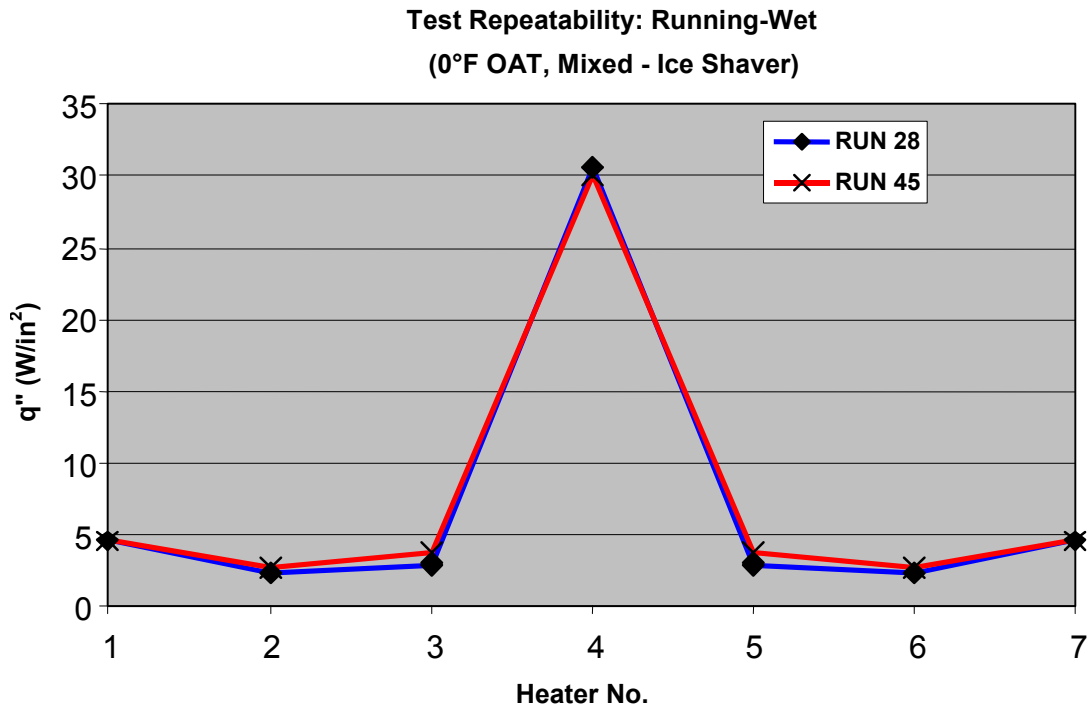


FIGURE 17. TEST REPEATABILITY (RUNNING-WET, MIX-SHAVER, 0°F)

7.2.2 Evaporative Anti-Icing.

Operation in evaporative anti-icing mode consisted of controlling all the heaters such that the surface temperature is stabilized to 150°F. Due to the high collection efficiency in the stagnation region (heaters 4 and 11), the cooling rate was very high so the heaters could run at maximum power, which was near 31 W/in² at those locations. The exact value depended on the actual line voltage during the test. Despite this relatively high power density, the stagnation temperature never reached 150°F. This is due to the high cooling rate associated with the combination of convection, evaporation, and latent heat of fusion for cases where ice particles were present in the cloud.

All the results are presented for a TWC of 0.7 g/m³ unless otherwise specified (see table 1). The total power was computed in each case by summing the power of all 14 heaters. Comparison of all the results revealed that the maximum total power occurred in the case of fully evaporative anti-icing mode in a cloud of supercooled liquid water only at 0°F ambient temperatures. To simplify the comparison between the different cases presented, the total power in each case was normalized to the case of maximum power already mentioned.

The following terms are used in the figure 18:

- Spray Bars indicates only supercooled liquid water cloud.
- MixGun indicates a mixed-phase condition with 50% supercooled water content and 50% ice particles from the snow gun.
- MixShaver indicates a mixed-phase condition with 50% supercooled water content and 50% ice particles from the snow gun.
- Shaver indicates fully glaciated icing conditions using the ice shaver.
- Gun indicates fully glaciated icing conditions using the snow gun.
- Gun low-LWC similar to Gun but only half the IWC, that is 0.3 g/m³ only.
- Dry indicates convective cooling for dry condition data, shown here for reference.

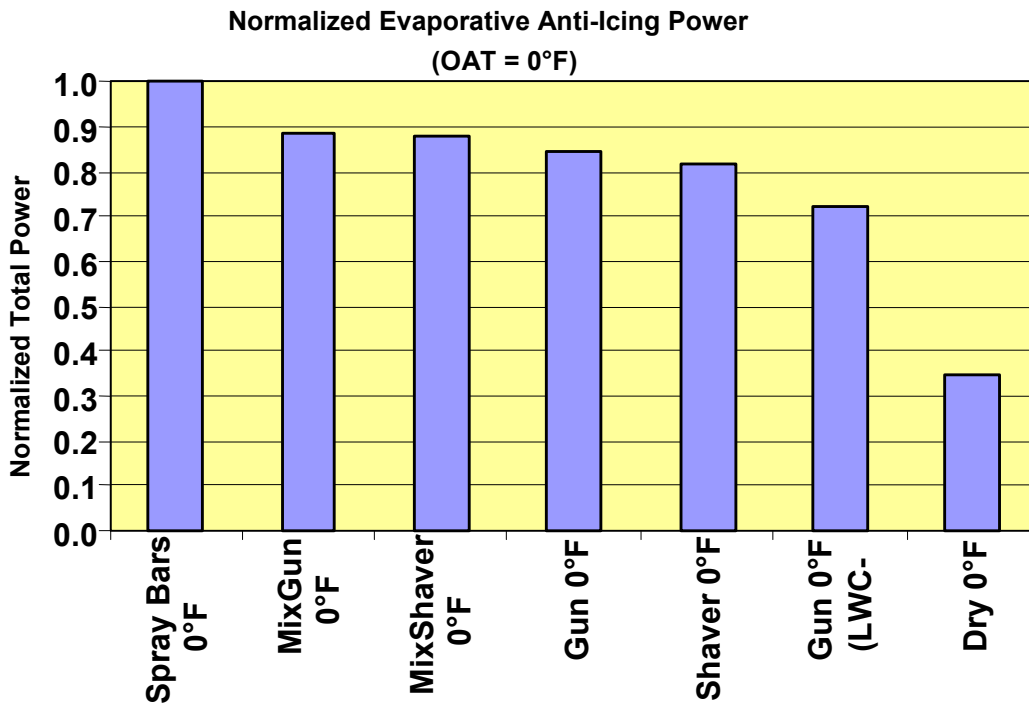


FIGURE 18. SUMMARY OF NORMALIZED EVAPORATIVE TOTAL POWER AT 0°F

The summary of results for the evaporative anti-icing cases at 0°F ambient temperature is shown in figure 18, where the normalized total powers relative to the spray bars (supercooled liquid only) are illustrated. The general trend observed in this figure suggests that the maximum power in a decreasing order for the evaporative cases is as follows:

- An all supercooled liquid water cloud (generated by the spray bars).
- Mixed-phase icing condition, equally from the snow gun and ice shaver.
- Fully glaciated conditions with ice particles only. The difference between the ice shaver and the snow gun is within the expected variance.
- Low ice particle content simulated with the snow gun ($TWC = IWC = 0.3 \text{ g/m}^3$).
- The dry convective conditions as presented for reference.

Looking at the actual distribution of each of these individual powers sheds more light on the effects of ice particles present in the cloud. Figure 19 illustrates the power-density distributions corresponding to evaporative anti-icing mode at 0°F ambient temperature. Recall that the case labeled Gun low-LWC corresponds to ice crystals only at 0.3 g/m^3 . This case was considered to validate the entire simulation/control process and to ensure that the correct trend in power reduction is obtained for that case. There are some interesting phenomena to note:

1. Power densities required to maintain the desired surface temperature for the liquid and mixed-phase conditions did not significantly differ in the vicinity of the model's stagnation region, heaters 3 through 5, even though the initial liquid water content of the mixed-phase conditions were half of that for the liquid condition. Lower power densities required for the glaciated conditions, relative to the liquid condition, are discernible, but they are significantly greater than the power density required for the dry condition. These results indicate that heat is being consumed to melt and evaporate some of the ice particles.
2. Power on downstream heaters, specifically nos. 2 and 6 (or nos. 9 and 13), are reduced in the case of mixed or glaciated conditions compared to the supercooled water case. This could be a thermal indication of water shedding downstream due to splashing caused by the relatively large and heavy ice particles impacting the local water film. Partial melting occurs in the stagnation region, and the ice particles cause some splash-off of surface water. However, away from the stagnation region, the ice particles tend to induce water shedding more efficiently, removing liquid water that might exist as a result of local direct impingement from supercooled droplets or runback that might come from upstream locations. That seems to be certainly the case, because the power at those locations was almost identical to the dry convective case, as seen in figure 19. However, following those heater zones are the aft-most heaters (nos. 1 and 7), which seem to exhibit an increase in power compared to the dry convective case. This could be a result of a possible re-impingement phenomenon from the splashing and bouncing effects that occur at the stagnation region. Another possibility is purely a stronger transition to a turbulent flow as a result of the upstream surface activities. For glaciated conditions, more particles bounce off the surface leaving only a thin water film resulting from the melting process. Moreover, the impinging ice particles further reduce the water film through the splashing phenomenon and by not adhering to the heated surface downstream of the stagnation region.

- The power required on the hilite, heaters nos. 4 and 11, is near 31 W/in^2 . This corresponds to the maximum heater design power at a line voltage of near 120 volts. In those cases, the hilite heaters ran below the specified surface temperature of 150°F , as discussed earlier.

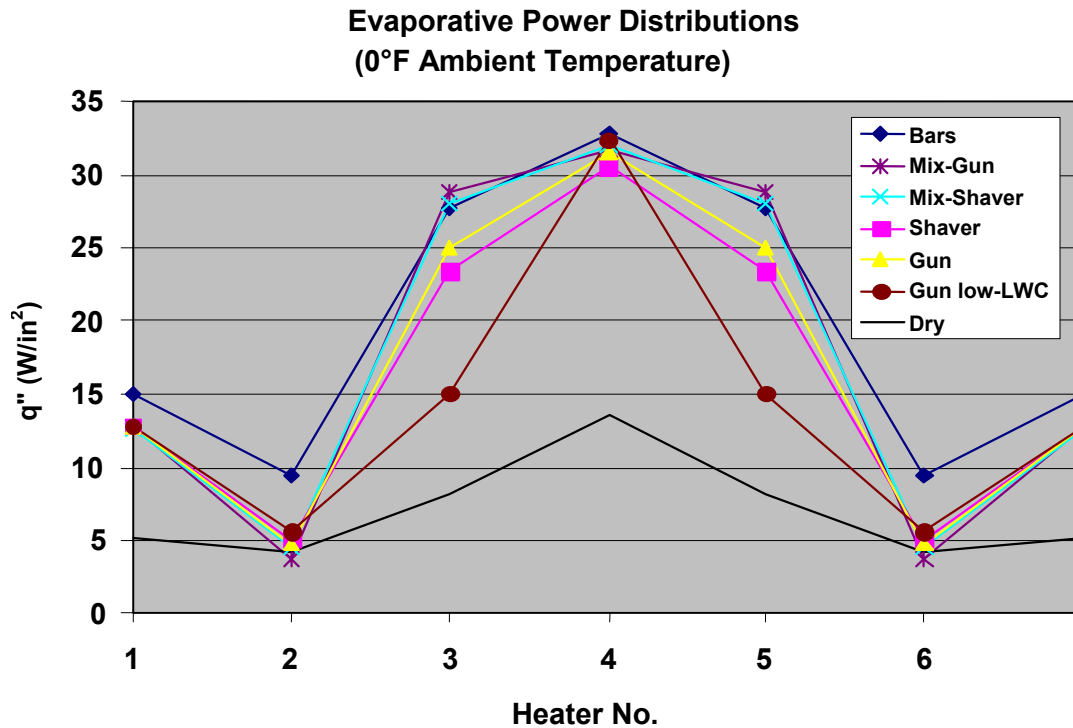


FIGURE 19. EVAPORATIVE POWER DISTRIBUTIONS AT 0°F

Similarly, the results corresponding to evaporative anti-icing mode at a warmer ambient temperature, 12°F , are shown in figures 20 and 21. The trend observed here is identical to the colder case illustrated in figures 18 and 19. Also, the respective normalized powers are slightly lower due to the decrease in the convective and evaporative losses at the warmer condition. This indicates that the results are very consistent and meaningful. Note that the required lower power density levels, the power densities required to obtain the desired surface temperature for the liquid and mixed-phase conditions are significantly different in the vicinity of the model's stagnation region, heaters 3 through 5. Less power is required for the mixed-phase conditions, suggesting that some of the ice particles are not being melted or that the water film thickness in that area is less than that for the liquid condition.

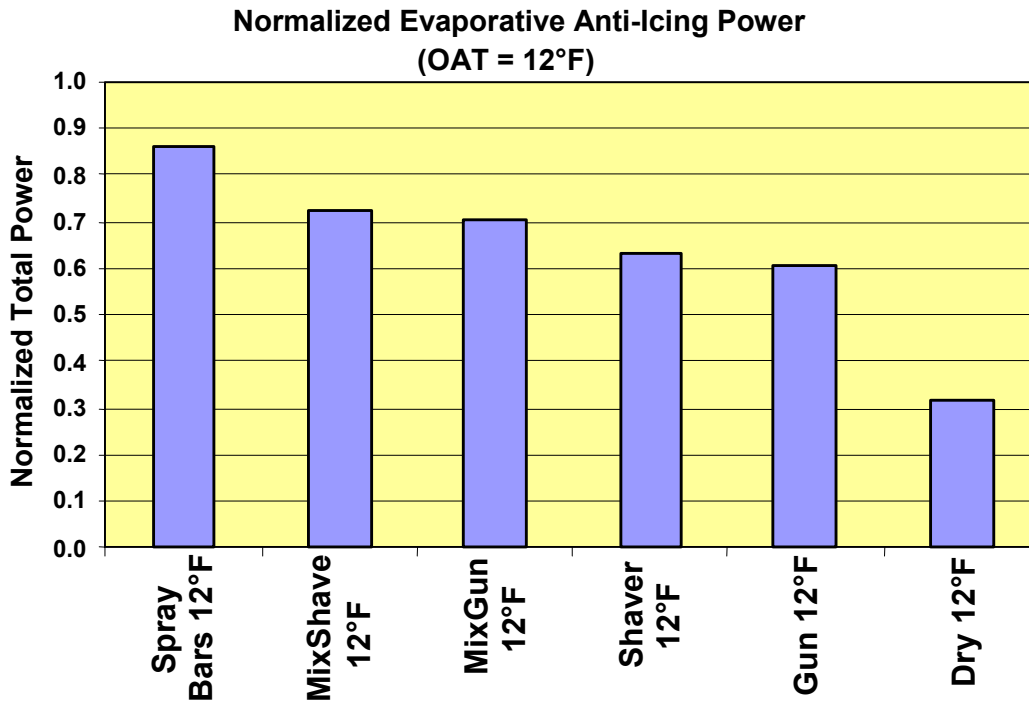


FIGURE 20. SUMMARY OF NORMALIZED EVAPORATIVE TOTAL POWER AT 12°F

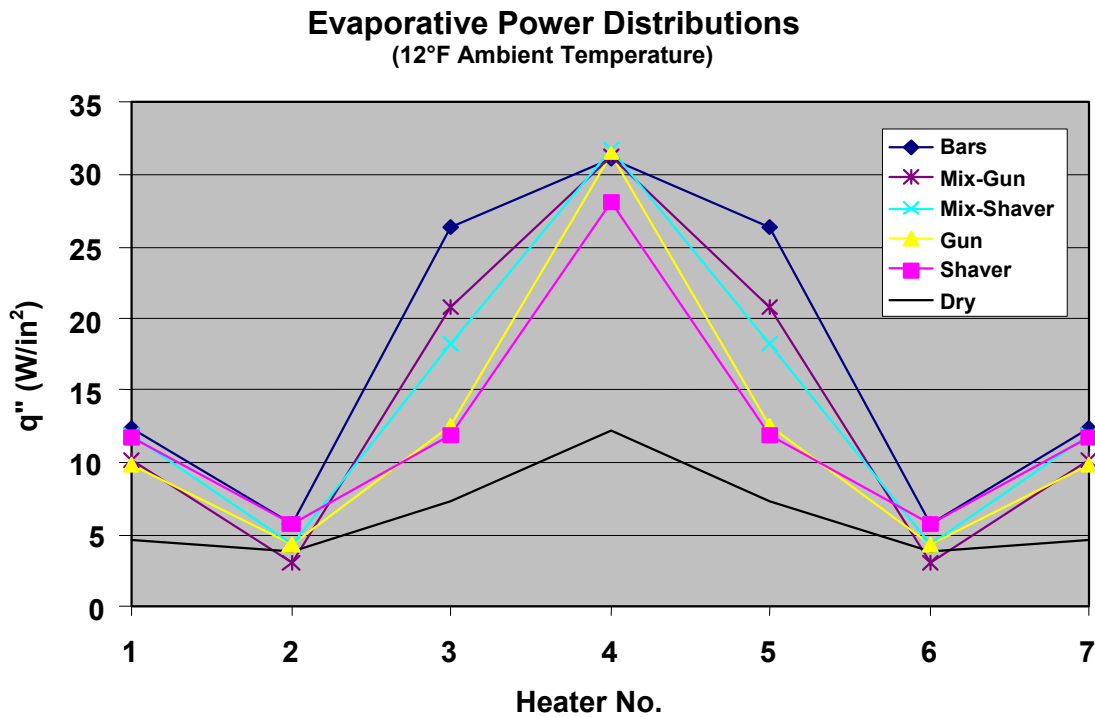


FIGURE 21. EVAPORATIVE POWER DISTRIBUTIONS AT 12°F

Also, note that the power density required for the glaciated conditions at the lower ambient temperature is closer to the dry model values, suggesting less melting of the ice particles. The water film shedding effects are more visible in figure 21 in the heated regions just downstream of the hilite than in figure 19 for the 0°F case. This is a result of the lower convective cooling in the warmer ambient case. Note that the differences between cases where the ice particles were generated using the snow gun versus the ice shaver are small and could be associated with the uncertainty in the IWC calibration as well as the small difference in ice particle sizes and shapes.

Although the surface temperature corresponding to heater 4 is colder than the adjacent heater zones, the heater element was much higher in temperature due to the high thermal gradient resulting from the local high power density, which explains the chordwise heat transfer.

7.2.3 Running-Wet Anti-Icing.

Now consider the running-wet anti-icing cases. Figure 22 illustrates the normalized total power at 0°F ambient temperature. Clearly, the total required power was much less than the equivalent values in the evaporative cases shown in figure 18. The trend shown here indicates that the power required in decreasing order corresponds to the mixed-phases, followed by the fully glaciated and supercooled droplet clouds. This trend indicates that more heat was being consumed during the mixed-phase conditions, suggesting that relative to the heat being consumed by the liquid condition, more heat is being consumed in the mixed-phase condition to melt the impinging ice particles even though some of the thinner surface water film is being shed due to the splashing caused by the ice particles.

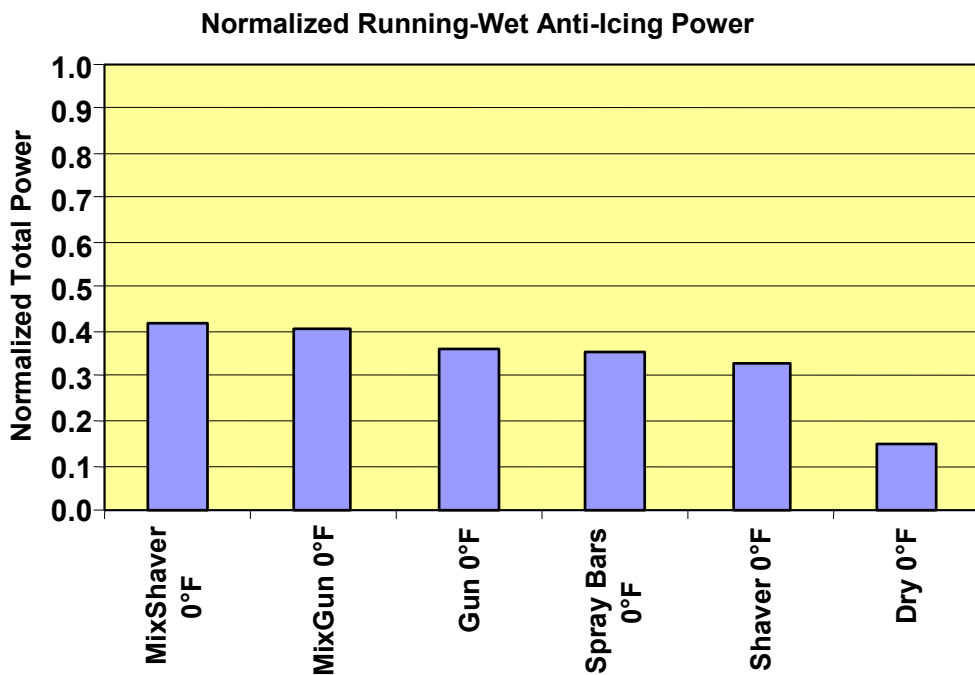


FIGURE 22. SUMMARY OF NORMALIZED RUNNING-WET TOTAL POWER AT 0°F

Detailed inspection of the actual power distributions shown in figure 23 indicates that for most running-wet cases, the power on the hilite is also at the maximum available, as in the evaporative cases. Notably, the heaters just downstream of the hilite required very little heat in mixed and glaciated conditions. Note the following possible contributing factors:

1. The ice accumulation on the hilite required high power as a result of the additional latent heat of fusion necessary to melt the ice crystals. Some of the heat generated on the hilite conducts in the chordwise direction to adjacent heaters, which tends to decrease the power required by the latter heaters. Once again, the chordwise heat transfer is explained by the fact that although the surface temperature corresponding to heater 4 is colder than the adjacent heater zones, the heater element was much higher in temperature due to the high thermal gradient resulting from the local high power density.
2. Immediately downstream of the stagnation region, heater 4, the power density required for the mixed-phase conditions are similar to that required for the all-liquid condition. However, the power density required for the glaciated conditions is similar to that for the dry model condition at those downstream locations, suggesting little or no heat being transferred to the ice particles at the lower model surface temperature.
3. Splashing caused by the relatively large and heavy ice particles has reduced the local water film thickness for the initially thinner film for the mixed-phase conditions (compared to the all liquid condition). For glaciated conditions, a few ice particles may have been melted by the lower heater surface temperatures resulting in a thin water film. The impinging ice particles further reduce the water film for this condition through the splashing phenomena and the particles do not adhere to the heated surface downstream of the stagnation zone. However, it is clear from figure 23 that some of the ice adheres to the stagnation as a result of the local high power density required due to the latent heat of fusion to melt the ice.

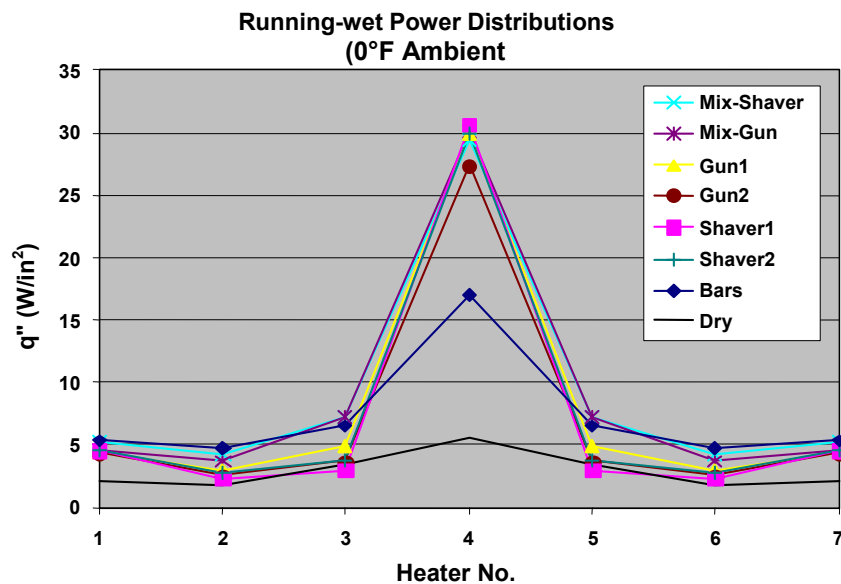


FIGURE 23. RUNNING-WET POWER DISTRIBUTIONS AT 0°F

Finally, the results corresponding to running-wet cases at 12°F ambient temperature are shown in figures 24 and 25. The trend observed here is similar to that of the 0°F case as far as the power distributed and erosion effects. Clearly, the normalized powers shown in figure 24 have decreased compared to the previous colder case. The same argument could be made to the actual power densities in each of the icing conditions. The erosion effects in the downstream heater region (heater nos. 2 and 6) are clear when comparing the power densities to the corresponding dry convective values, as shown in figure 25.

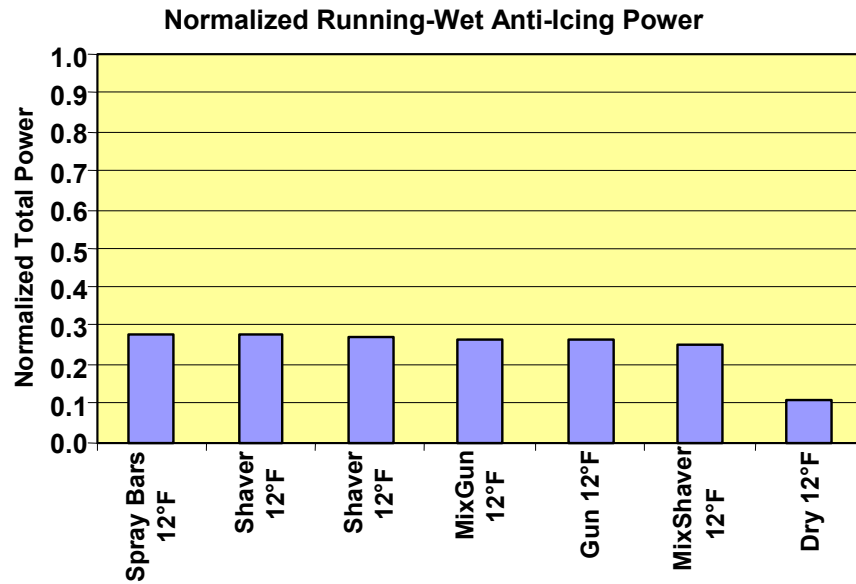


FIGURE 24. SUMMARY OF NORMALIZED RUNNING-WET TOTAL POWER AT 12°F

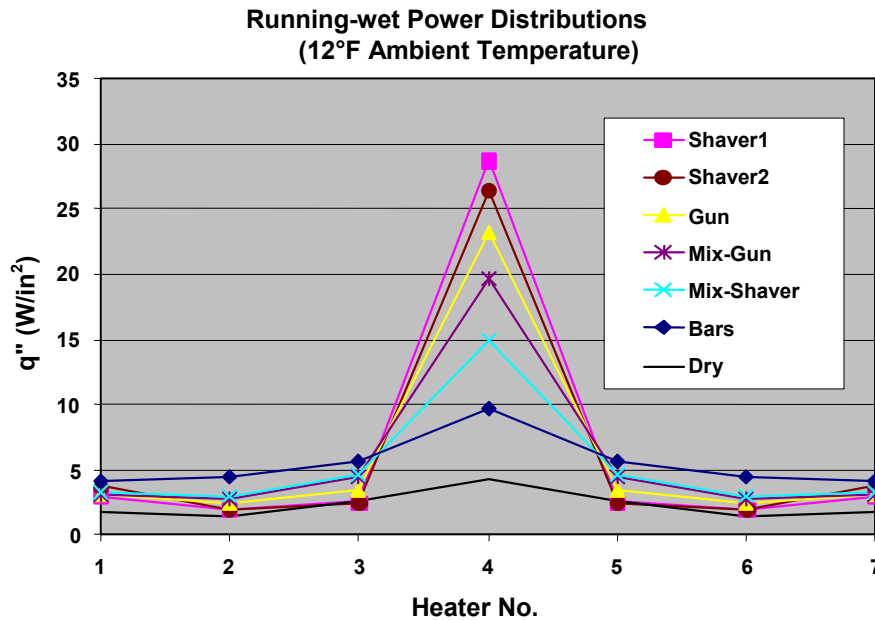


FIGURE 25. RUNNING-WET POWER DISTRIBUTIONS AT 12°F

Figure 26 illustrates an ice ridge that formed immediately downstream of the heated zones on the upper surface during run 26. This is a running-wet condition in supercooled liquid water cloud at 0°F ambient temperature. As discussed earlier, the amount of runback is reduced in mixed-phase conditions for the same TWC and icing exposure duration. Running-wet systems are not usually employed on wings and tails. They are more common in engine inlet ducts. Based on this research, design engineers should be cautious when using running-wet systems where applicable.

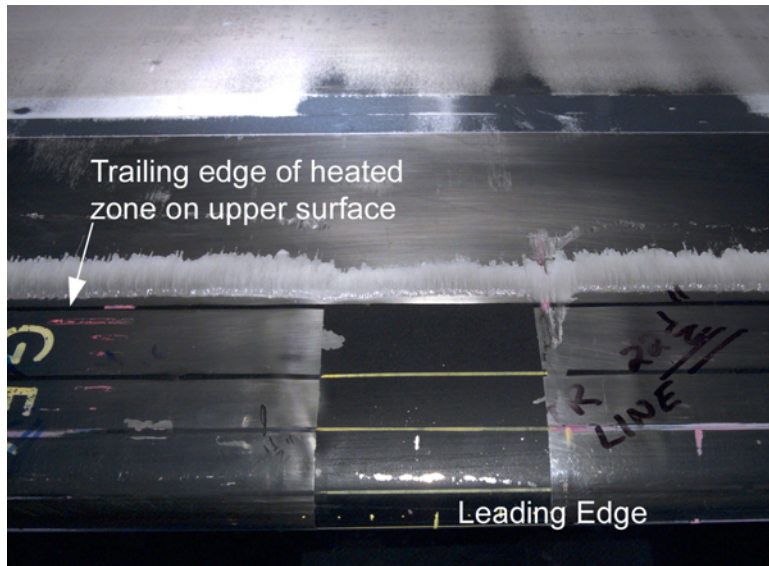


FIGURE 26. ICE RIDGE FORMATION DOWNSTREAM OF HEATED ZONE FOR RUNNING-WET SYSTEM

8. CONCLUSIONS.

A new capability to simulate glaciated and mixed-phase icing conditions was developed and demonstrated in the Cox & Company LeClerc Icing Research Laboratory (LIRL) tunnel. This capability proved to be very useful in conducting research studies in repeatable and controllable environments. This would have been very difficult to achieve in flight where it is almost impossible to encounter the same stabilized conditions to compare results between different anti-icing operating modes at different temperatures.

An experimental program, sponsored by the Federal Aviation Administration, was conducted to quantify the effects of mixed-phase and glaciated icing conditions on the power requirements of thermal ice protection systems. The investigation was limited to a lifting surface at zero degree angle of attack.

Visualization techniques and test methods were developed and demonstrated during this test process. Erosion effects were evident, especially in glaze icing conditions as well as cases where the surface was heated. Resulting accretions on unheated surfaces were usually smoothed by the presence of ice particles in the cloud and tended to be opaque white, as is common in rime cases. Erosion effects were documented through ice tracings and visual data, as well as thermal data.

Generally speaking, the performance of the evaporative thermal system on the model did not seem to be adversely affected by the presence of ice particles in the cloud. In fact, purely liquid clouds required more heat than mixed-phase or glaciated conditions with the same total water content. The lower power density requirements for the mixed-phase and glaciated conditions may have resulted from some of the ice particles bouncing from the surface without melting and from loss of water from the heater surface water film due to splashing caused by the impacting ice particles.

Ice protection systems operating at temperatures slightly higher than the freezing point of water, typical of running-wet systems, require less power than evaporative systems. This is because the aim is to prevent ice forming on the surface but not fully evaporating it. Running-wet power requirements increase as the ambient air temperature decreases. In mixed-phase icing conditions, additional power is required to offset the heat of fusion for melting the impinging ice particles. However, in this test, the large, relatively heavy, ice particles apparently cause shedding of the water film on the ice protection system surface through the dynamics of splashing as the ice particles strike and bounce from the airfoil's surface. The reduced water film thickness aft of the airfoil's stagnation point tended to offset the effects of the ice particles that impinge and adhere at the leading edge of the model. Consequently, the overall power required by the running-wet ice protection system was practically unchanged between all-liquid and mixed-phase conditions. However, in the running-wet mode, the local power density was much higher around the stagnation area in the mixed-phase conditions compared to the purely liquid conditions. This is a result of the power required to offset the heat of fusion necessary to melt the impacting ice particles that either fully or partially stick to the surface. In all running-wet modes, runback ice was observed to freeze near the trailing edge of the protected surfaces, with the formation of an ice ridge resulting from the buildup of ice from subsequent runback water on initial runback ice formation.

The test methodologies and imaging tools developed in this program can be transferred to an aircraft test bed for flight studies in natural icing conditions. However, extensive data should be collected to be conclusive. An actual flight test program might prove very difficult due to the high fluctuations in ambient conditions.

Results of this investigation do not resolve all questions concerning whether or not mixed-phase icing conditions are sometimes more hazardous to flight than purely liquid water conditions with the same liquid water content. Results of the current testing can be used by manufacturers to investigate the mixed-phase icing hazards associated with specific airplane components and designs. It would be valuable if this investigation were augmented to include additional testing parameters such as operational angle of attack, higher airspeed, and other total water contents and liquid water droplet size.

It is important to note that the effects on the operation of turbine engines and air data system probes remain to be investigated. Other applications for operation in mixed-phase icing conditions could be studied in the tunnel, such as investigations to include heated instrumentation and air data probes. Also, if the ice shaver is used, higher-speed effects and better close-up imaging can be conducted in Test Section-1 of the Cox LIRL tunnel, since data of this study was limited to the Test Section-2 maximum speed of 120 mph.

The studies were conducted with currently available simulation methods and visualization techniques. Although the ice particles simulated here may represent only a small percentage of the types that may exist in nature and direct correlations to nature may not be possible, the trends observed in the tunnel are expected to be valid in flight during natural icing encounters. This is especially true in the case of heated surfaces.

9. REFERENCES.

1. “FAA Inflight Aircraft Icing Plan,” U.S. DOT, Federal Aviation Administration, April 1997.
2. Riley, J.T., “Mixed Phase Icing Conditions: A Review,” FAA Specialists’ Workshop on Mixed Phase and Glaciated Icing Conditions, Atlantic City, NJ, December 2-3, 1998.
3. Proceedings of the FAA Specialist’ Workshop on Mixed-Phase and Glaciated Icing Conditions,” held December 2-3, 1998, June 1999.
4. Miller, D.R., Wright, W.B., and Al-Khalil, K.M., “Validation of Thermal Ice Protection Computer Codes: Part 1—Program Overview,” AIAA 35th Aerospace Sciences Meeting, Reno, NV, January 1997, AIAA Paper 97-0049.
5. Wright, W.B., Miller, D.R., and Al-Khalil, K.M., “Validation of Thermal Ice Protection Computer Codes: Part 2—The Validation of LEWICE/Thermal,” AIAA 35th Aerospace Sciences Meeting, Reno, NV, January 1997, AIAA Paper 97-0050.
6. Al-Khalil, K.M., Horvath, C., Miller, D.R., and Wright, W.B., “Validation of Thermal Ice Protection Computer Codes: Part 3—The Validation of ANTICE,” AIAA 35th Aerospace Sciences Meeting, Reno, NV, January 1997, AIAA Paper 97-0051.